

# Thermal comfort, daylight, and energy performance of envelope-integrated algae-based bioshading and static shading systems through multi-objective optimization

Maryam Talaei <sup>a,\*</sup>, Hamed Sangin <sup>b</sup>

<sup>a</sup> Faculty of Architecture and Urban Planning, Ferdowsi University of Mashhad, Mashhad, Iran

<sup>b</sup> Department of Environment, Land and Infrastructure Engineering (DIATI), Politecnico di Torino, Turin, Italy

## ARTICLE INFO

### Keywords:

Bioshading  
Microalgae photobioreactor  
Multi-objective optimization  
Thermal comfort  
Energy efficiency  
Daylight

## ABSTRACT

Energy-efficient envelopes integrated with different shading devices, as noticeable passive design strategies, have been of great interest for research studies. However, there is a lack of attention on optimizing envelope-integrated novel algae-based bioshading systems (ABBS) in comparison with other shading devices to enhance buildings' sustainability-oriented performances. Integrating microalgae culture system with building façade as a state-of-the-art bioshading system is among recent developments in high-performance architecture. Although, challenges/limitations concerning different performances of this technology have not been extensively addressed. The present study conducts a multi-objective optimization framework to investigate the Thermal Comfort Percentage (TCP), Useful Daylight Illuminance (UDI), and Energy Usage Intensity (EUI) in a school building to evaluate the relationship between the performance objectives and design variables (shading characteristics, window-to-wall ratio (WWR)) through comparing different static shading systems and ABBS in the hot (BSh) and cold semi-arid (BSk) climates. The Technique for Order of Preference by Similarity to Ideal Solution (TOPSIS) method was also applied to determine the best design options within Pareto frontiers. Results demonstrated that horizontal louver by 128.52 % TCP, 15.10 % UDI improvement in south-oriented façade in BSk, and overhang with fin (OF) by 18.99 % EUI reduction in southern façade in BSh climates contribute the most to enhance the objective metrics. Also, ABBS was not a stand-first system to enhance all the objective metrics compared to the other shading systems in none of the examined climates. Sensitivity analysis indicated that WWR has the most significant positive impact on EUI compared to the other studied metrics in almost all design options.

## 1. Introduction

Regulating energy consumption and enhancing indoor environmental comfort are regarded as fundamental requisites for realizing low-carbon and green buildings [1]. Hence, it is a key point to improve daylight and thermal comfort and reduce energy use in a building. Accordingly, decisions in early-stage design play a considerable role in enhancing energy saving and user comfort, which can be achieved through the multi-objective optimization (MOO) process [2,3]. Meanwhile, as an interface between indoor and outdoor environments, building envelopes noticeably contributes to energy-saving in buildings and realizing sustainable architecture [4].

\* Corresponding author.

E-mail addresses: [p.barboni60@gmail.com](mailto:p.barboni60@gmail.com), [m.talaei@ferdowsi.um.ac.ir](mailto:m.talaei@ferdowsi.um.ac.ir) (M. Talaei).

**Table 1**  
Key research on MOO of educational building.

Ref	Location	Climate Type	Optimization Objective	Design Parameters	Shading Type	Simulation and Optimization Tools and Methods
[44]	Qeshm Island, Iran	Hot desert climate (BWh)	Total energy consumption, predicted mean vote (PMV), percentage of people dissatisfied (PPD), UDI, Spatial daylight autonomy (sDA)	Building orientation, number/depth/angle of shades, glazing material, WWR, the distance between shades	Horizontal shading device	Honeybee, Ladybug, Genetic algorithm
[29]	Tianjin, China		Energy demand, summer discomfort time, UDI	Orientation, depth of classroom/corridor, glazing ratio of the interface, glazing material, shading type	Venetian blinds & roller shading	Ladybug tools, Octopus
[24]	Nanjing, China	Humid subtropical (Cfa)	Annual energy consumption (Artificial lighting, Heating, Cooling, Fresh air), thermal comfort, cost	Solar absorptivity/ Thickness/Thermal conductivity of external wall, WWR, fin (depth/angle), overhang (depth, angle/height)	Overhang, fin	Artificial neural network (ANN) model + multi-objective particle swarm optimization (MOPSO) + NSGA-II EnergyPlus + Python
[28]	Nanjing, China	Cfa	Annual total power consumption (TES), UDI, Proportion of thermal comfort duration (PT), Life cycle cost	Variables pertinent to wall, photovoltaic, window, and shading system	Outer Corridor/Overhang	NSGA-II & Segregative Genetic Algorithms -Q
[25]	Nanjing, China	Cfa	TES, PT, UDI	WWR, window type, Shading, wall & and roof thermal characteristics, roof skylight	Overhang	MOPSO, MOGA, NSGA-II algorithm
[30]	Nanjing, China	Cfa	Energy, Life cycle carbon emissions	Site layout, Geometry, Structure, Envelope, Shading type, Window glass type, WWR, Energy system	Static (Overhang, Fin), Moveable (Louver, Curtain)	DesignBuilder, Metha model (ANN), Segregative Genetic Algorithms
[45]	Denver, Baltimore, Miami, Los Angeles	cold, mixed-humid, hot-humid, and hot-dry	Energy use, UDI (horizontal & vertical daylighting levels)	Classroom Geometry, Window features, WWR, Orientation	-	Ladybug, Honeybee, Octopus
[46]	Tehran, Iran	Cold semi-arid (BSk)	UDI, DA (Daylight autonomy), Daylight Glare Probability (DGP), Annual Sunlight Exposure (ASE), Annual thermal energy use intensity (TEUI), Annual thermal comfort ratio (CTR)	Orientation, Wall angle, Number of Window, WWR, Glazing material	-	Ladybug, Honeybee, Octopus
[26]	Tehran, Iran	BSk	UDI, ASE, DGP, EUI, CTR, Electrical power produced by PVs	Shading characteristics	Photovoltaic integrated shading device, Louver	Ladybug, Honeybee, Octopus
[3]	Biskra, Algeria.	BWh	UDI, DA, Thermal adaptive comfort percentage, EUI	WWR, wall materials, glass types, shading	Vertical louver	Ladybug, Honeybee, Octopus
[33]	Montreal, Canada	Humid continental (Dfb)	Overheating hours, heating, and artificial lighting energy use	Shading type/ characteristics, WWR, Window Opening Ratio, night cooling, wall and cool roof U-value, roof solar reflectance, infiltration	Exterior shading (overhang, screen shading), Interior shading (blind rolls)	DesignBuilder, EnergyPlus, NSGA-II algorithm, jEPlus + EA
[47]	Warsaw, Poland; Bangkok, Thailand	Dfb; Tropical savanna (Aw)	Annual energy demand, CO <sub>2</sub> concentration, PPD	Indoor temperature set points for opening control, thermostat set points, window opening area	-	SketchUp, EnergyPlus, NSGA-II algorithm, jEPlus + EA
[48]	Tehran, Sari, Iran	BSk, Hot-summer Mediterranean (Csa)	UDI, ASE, sDA	WWR, Shading characteristics	Light-shelf	Ladybug, Honeybee, Octopus

(continued on next page)

Table 1 (continued)

Ref	Location	Climate Type	Optimization Objective	Design Parameters	Shading Type	Simulation and Optimization Tools and Methods
[31]	Sabzevar, Iran	Bsk	DGP, UDI, DA, Lifecycle energy/Cost/assessment LCE, LCC, LCA Annual Energy consumption	Shading systems and their material	Overhang, Louver (vertical&horizontal), light shelf, Egg-crate	Ladybug, Honeybee, Wallacei X, OpenLCA,
[20]	Shanghai, China	Cfa	Spatial glare autonomy (sGA), Spatial daylight vote autonomy (sDVA)	Shading type& characteristics, Orientation	Perforated aluminum sheet, slats, serrated windows	ANN, NSGA-II, Ladybug, Honeybee, Wallacei X
[35]	Nanjing, China	Cfa	PV production, Radiation, Daylight	Shading characteristics	Photovoltaic shading system	Ladybug, Honeybee, Octopus
[34]	Nanchang, China	Cfa	UDI, sDA, DGP, Window view satisfaction, Luminance ratio of blackboard and desktop, Uniformity of ratio, and illuminance	Shading, Orientation, Perforated panel-to-window ratio, Perforated percentage, hole arrangement	Overhang, Vertical shading, Perforated panel	NSGA-II, Grasshopper, Daysim, Radiance, EnergyPlus
[6]	Guangzhou, China	Cfa	UDI, Annual energy demand, PMV	Building Geometry, Orientation, Shading and Glazing type, Wall construction, WWR	Horizontal and vertical shading, Egg-crate	NSGA-II, Grasshopper, Ladybug tools, EnergyPlus
[32]	Tallinn, Estonia	Dfb	Primary energy, Spatial Disturbing Glare(sDG), sDA Quality views	Shading depth, rotation angle, Distance between shading slats, height	Fins, Horizontal/vertical louvers, Eggcrate, Light shelf	Rhinoceros, Grasshopper, Radiance, Opossum, Radial Basis Multi-Objective Optimization

Therefore, different studies have focused on optimizing building envelope characteristics and its components to improve energy efficiency, thermal comfort, and daylight level in the early design stage of a building [5–8]. Achieving a balance between daylight and energy performance in school buildings is of utmost importance since 70 % of students' time is spent in the classroom [9], and they are less adaptable and more susceptible to environmental conditions than adults [10]. The direct relationship between the daylight level and energy efficiency, as well as the impact of the indoor environment on students' learning ability, well-being, and healthiness [10, 11], highlights the role of controlling and making a balance between building performance metrics such as daylighting, thermal-/visual/acoustic comfort and energy efficiency in the early-stage design of school building. Regulating lighting environment is also regarded as a key factor in classroom design due to its impact on students' visual quality [12], learning performance [9], hormonal production and body growth [13], and the circadian clock [14]. Moreover, different studies investigated the relationship between students' health, academic performance, and indoor thermal conditions [9,15,16]. Meanwhile, shading devices as key components of the building envelope can significantly improve indoor thermal conditions, visual comfort, decreasing glare, and specifically building energy consumption through controlling daylight level [17–19]. Hence, they are considered as noticeable passive solutions to pave the route towards sustainable and energy-efficient buildings. Although numerous shading devices are accessible and applied to building envelope, they cannot always perform efficiently, and it is also traditionally problematic to select the best options and strategies [20]. Accordingly, different research has performed MOO studies on building envelope characteristics and components, including fenestration/glazing features, shading systems, geometry, and material [2,19,21–23], although comparing different shading devices to achieve the most suitable passive solutions have not been addressed, comprehensively, by previous research especially in different climate zones considering educational buildings.

Xu et al. [24] proposed a two-stage MOO procedure coupled with a meta-model to improve daylight, thermal comfort, energy-saving, and cost of school buildings in China considering the building envelope characteristics, including shading features and energy systems as variables. Their method brings about significant advantages considering the results' validity, precision, and diversity due to applying various MOO algorithms. In another study [25], they also took a three-stage MOO design process to achieve effective and precise optimization results in the classroom considering three objective functions: energy consumption, students' thermal comfort, and daylighting. The research demonstrated the superiority of electrochromic windows to standard windows regarding the studied indices. It also showed the advantages of Non-dominated sorting genetic algorithm II (NSGA-II) compared to multi-objective particle swarm optimization (MOPSO) and Multi-objective genetic algorithm (MOGA) in most aspects. Noorzai et al. [26] proposed a multi-objective design method to optimize a novel designed PV-integrated fixed vertical shading, which could enhance the students' thermal and visual comfort and increase the energy efficiency of a classroom up to 20 % in Iran. Park et al. [27] explored the energy performance of a Phase change material (PCM)-integrated shading system to improve energy efficiency and thermal comfort in an educational building in South Korea. The results indicated 44 % cooling energy reduction and a 34 % increase in thermal comfort hours. Moreover, different research has scrutinized the role of miscellaneous window systems and shading devices such as overhang [28], Venetian blinds/roller shading [29], louver, fins [30], egg-crate [31,32] fixed/moveable screen shading [33], perforated panel [34], PV shading system [35] on environmental performance of the educational building. Research also focused on adaptable shadings [36–38], smart windows [39] like Gasochromic [40], photochromic [41], energy-generating glazing [42], microalgae bio-adaptable windows [43] applied in various building types. Table 1 outlines key research on the MOO of school building/envelope to improve

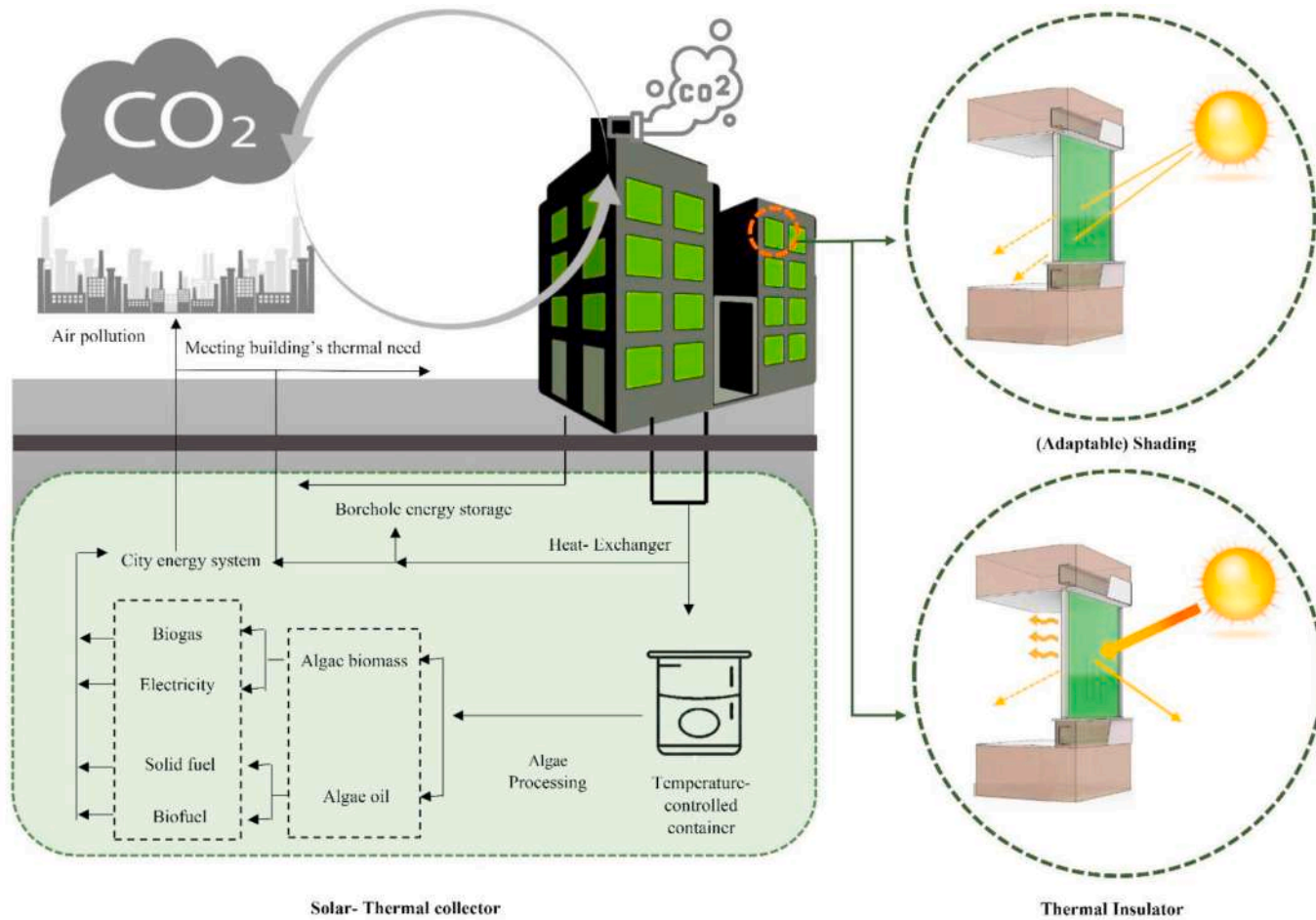
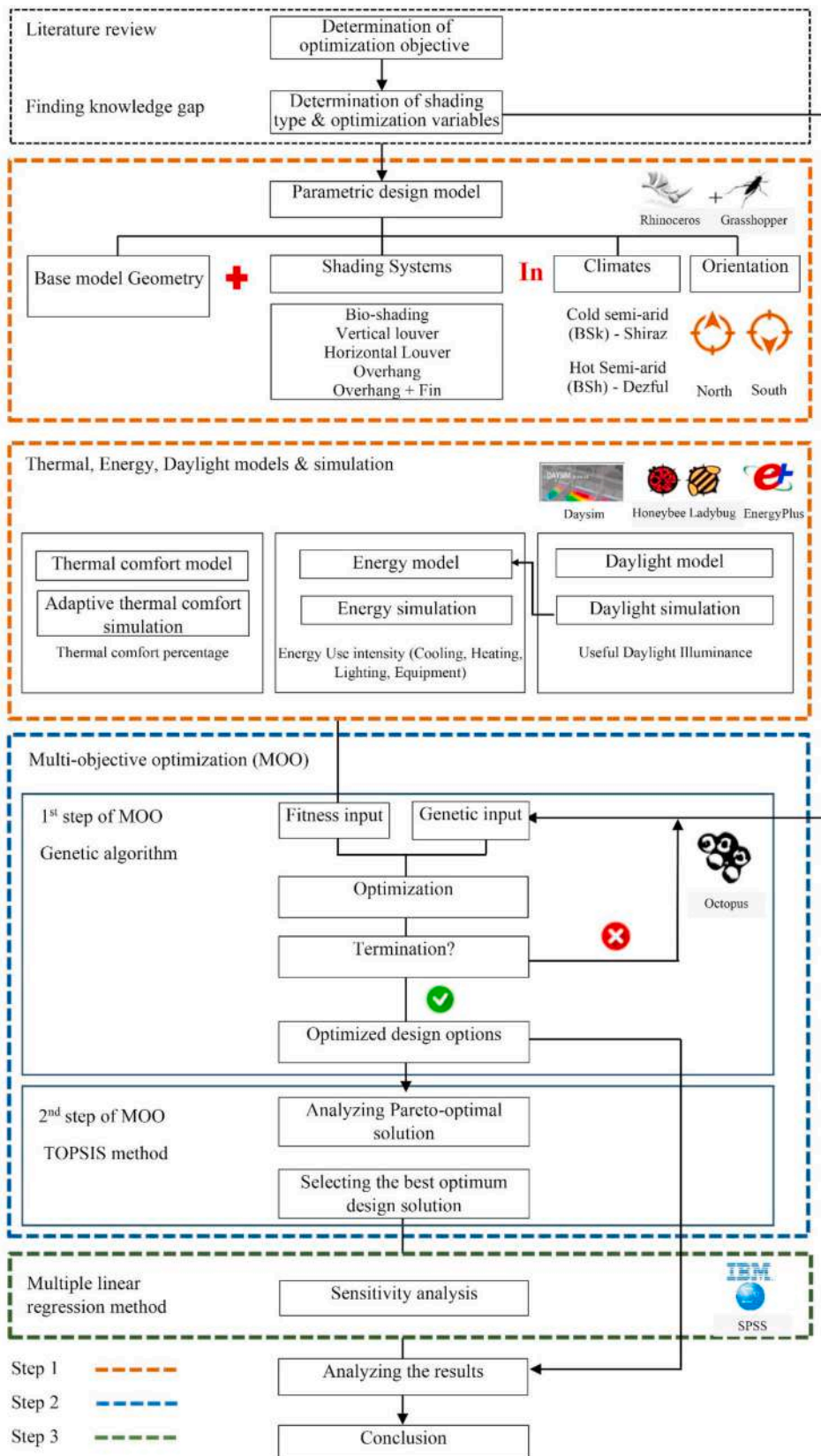


Fig. 1. Energy performance of algae façade system through solar-thermal systems, thermal insulator and shading.



(caption on next page)



Fig. 2. Research framework.

building different performance metrics. However, no previous study investigated the application of algae-based bioshading systems (ABBS) on thermal comfort, daylight, and energy performance of a school building in an early-stage design through the MOO design method and made a comparison with the common static shading strategies.

Accordingly, the present study is to investigate and compare the environmental performances of envelope-integrated microalgae shading system with that of different fixed exterior shading devices (FESD) in an educational building, in the semi-arid climate of Iran, which has not any precedent in the literature. Semi-arid climates have hot/warm summers, where shadings are critical passive strategies for controlling sun radiation and cooling energy demand.

1.1. Algae-based bioshading system

Integrating microalgae culture system known as a photobioreactor (PBR) with building façade provides significant bilateral advantages for both the building and the culture medium through thermal symbiosis [49]. Photobioreactor Facades (PBRF), as a state-of-the-art bio-façade technology, also potentially bestow energy saving [50], air pollution reduction [51,52], sound insulation [53] and wastewater treatment [54] to the building. Energy efficiency in PBRF is provided by solar thermal collectors, light-to-biomass converters that produce biofuel and heat, (adaptable) shading as well as thermal insulation [55] (Fig. 1). Microalgae, known as a newly-emerged building biomaterial, can interact with solar radiation and CO<sub>2</sub> in the air, which results in microalgae cell growth and denser culture density. The more the PBRF is exposed to solar radiation, the more culture concentration increases, which can regulate light transmittance through the panel. However, excessive sun radiation leads to photosaturation and photoinhibition, which is detrimental to cell growth [56]. Hence, light control is regarded as one of the key parameters in PBR design. Besides, microalgae growth and PBR design demand significant considerations including mixing, light, temperature, CO<sub>2</sub>, PH level and nutrients [57,58].

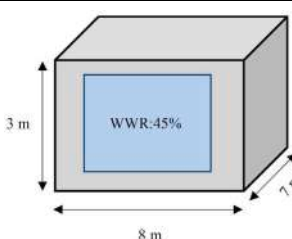
Different studies have focused on the thermal, energy, and daylight performances of PBRF [50,59,60]. Negev et al. [61] demonstrated the great energy-saving potential of microalgae window (MW), especially in south- and west-oriented windows compared to single- and double-glazed windows in the Hot-summer Mediterranean (Csa) climate. Talaei et al. [62] studied the effects of MW on the energy and daylight metrics of an office building through MOO in BSk climate. They also proposed a novel user-friendly bio-adaptable MW, which can regulate light transmittance through different culture medium heights [63]. Lo Verso et al. [64] presented PBRs as translucent and responsive screening elements, which can potentially regulate daylight penetration to the indoor space by adjusting medium concentration via a developed sensor-based control system. The proposed system provides sufficient visual comfort for a workspace used for different purposes. In the other study [43], the shading impact of the colored MW in light and heat regulation resulting in users thermal comfort in a Hot desert climate (BWh) was demonstrated. Despite the considerable advantages of integrating microalgae PBR with building façade, numerous challenges remain to be addressed by future studies, such as the high cost of the system, structure, and building regulation measurements, their environmental performances under different climate zones, etc [60, 65]. Besides, the daylight and energy performance of this innovative façade system has not been compared with single- and double-glazing windows in combination with different FESDs as common passive shading strategies. Also, no previous studies investigated the potential of MW in early-stage design through the MOO method to optimize daylight, energy, and thermal comfort indices, especially in educational buildings.

2. Material and method

The process of the present study can be described based on the following steps to investigate the optimum parameters and the studied objectives (Fig. 2):

First, the parametric simulated model was generated by Grasshopper, Rhino 3D modeling version 6 SR31, and the design variables have been identified to achieve the optimum quantification based on the defined building performance metrics. Besides, the base model's thermal comfort, energy, and daylight indices (Section 2.2), including north and south window orientations in Shiraz and Dezful, were measured. In this study, energy and daylight simulation have been conducted using Ladybug tools Version 1.6.0, which is

Table 2  
Construction and reflectance value of the model structure.

Base model	Construction and Model Structure		U-Factor (W/m <sup>2</sup> K)	R-Value (m <sup>2</sup> .K/W)	Reflectance values
	Roof	0.1 m Brick+ 0.2 m Heavyweight concrete+ 0.05 m Insulation board	0.481527	1.912975	-
	Wall	0.1 m Brick + 0.2 m Heavyweight Concrete+ 0.05 m Insulation board + Generic wall air-gap+ 0.019 m Gypsum board	0.426351	2.18173	(Interior wall) 50 %
	Floor	Acoustic tile + Generic ceiling air-gap+ 0.1 m lightweight concrete	1.170985	0.690229	(Interior floor) 20 %
	Ceiling				70 %
	Shading devices Earth surface				80 % 20 %

**Table 3**  
Weather data of Shiraz and Dezful.

			Dry-bulb temperature (C)	Relative humidity (%)	Wind speed (m/s)	Direct normal radiation (Wh/m <sup>2</sup> )	Diffuse horizontal radiation (Wh/m <sup>2</sup> )	Global horizontal radiation (Wh/m <sup>2</sup> )	Horizontal infrared radiation (Wh/m <sup>2</sup> )	Total sky cover (tenth)	Latitude, Longitude
Dezful	Hourly	Min	2.4	10	0	0	0	0	239	1	32.40°N, 48.38° E
		Max	51	100	12.9	934	409	1011	460	10	
		Average	24.69	42.46	1.82	279.36	58.11	234.68	339.76	1.82	
Shiraz	Hourly	Min	-9.4	10	0	0	0	0	154	0	29.62°N, 52.55° E
		Max	38.3	99	14.4	1016	444	1053	401	10	
		Average	16.40	38.15	1.31	307.78	58.14	255.89	278.62	1.66	

based on validated tools, including Radiance [66] and Daysim [67] as daylight simulation engines and EnergyPlus [68,69] and OpenStudio as energy simulator engines.

**Second**, multi-objective genetic optimization (MOGO) was applied to investigate the optimum solutions based on shading features and WWR as independent variables in two different climates, including Hot (BSh) and Cold semi-arid (BSk), to enhance the school building environmental performances. The TOPSIS method was applied in the next step of the MOGO to choose the absolute optimum design solution within the Pareto fronts.

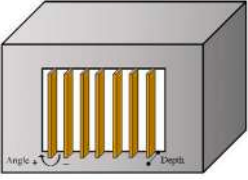
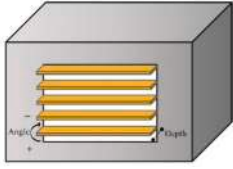
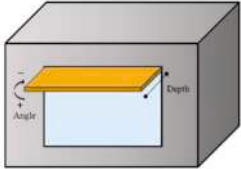
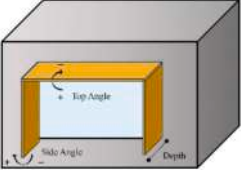
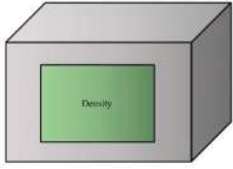
**Third**, the sensitivity analysis method based on linear regression was to examine and realize the relationship between the design parameters and the studied objective metrics.

**Finally**, validation was conducted to examine the accuracy of the simulation model based on a comparative method [70].

2.1. Defining the base case

The study case is a single-zone educational unit (Table 2) modeled based on typical classrooms in Iran proposed by The Organization for Development, Renovation and Equipping Schools (DRES). The unit with the dimensions of 7 m × 8 m × 3.5 m is north and south-oriented according to the DRES guidelines for Iran’s educational spaces to achieve more energy efficiency [48]. The base model has a diabatic façade with 45 % WWR and a center-located double-glazed window and adiabatic walls, whose properties, including thermal and reflectance features are presented in Table 2. The occupied period for the research base model is defined between 8 a.m. and 6 p.m. during a typical year with 0.35 ppl/m<sup>2</sup> number of people per unit of area. The cooling and heating setpoints were set as 26 and 20 °C, respectively, and the Daylight Illuminance setpoint was defined as 500 Lux. The HVAC system was defined as Ideal air load since it is the most suitable option in the early-stage design process regarding the cost of the calculation time [29,46]. Since educational

Table 4  
Value range of shading features.

Shading system/Variables	Variable ranges and characteristics			
	Depth (Increment 0.05 m)	Tilt angle (Increment 5°)		
V-louver 	0.1–1 m	0 ≤ θ(°) ≤ 180		
H-louver 	0.1–1 m	0 ≤ θ(°) ≤ 180		
Overhang 	0.1–1 m	0 ≤ θ(°) ≤ 180		
Overhang + Fin (OF) 	Vertical depth 0.1–1 m	Vertical angle 0 ≤ θ(°) ≤ 180 Horizontal angle 0 ≤ θ(°) ≤ 180		
Bioshading system (ABBS) 	Concentration	U-factor (W/m <sup>2</sup> K)	SHGC	VT
	20 %	4.9	0.40	0.45
	30 %		0.30	0.33
	40 %		0.20	0.17
	50 %		0.16	0.14
	60 %		0.13	0.11
	70 %		0.11	0.08
	85 %		0.09	0.06
	100 %		0.07	0.04
WWR	10 %–90 % (Increment 5 %)			



buildings in Iran are not tightly built, the infiltration rate per area is  $0.0003 \text{ m}^3/\text{s}\cdot\text{m}^2$  according to ASHRAE recommendation for Average buildings.

Shading strategies in the present study are FESD, including overhang, vertical/horizontal louvers, and overhang with fins (OF) deployed on a double-glazed window (3.2 U-value  $\text{W}/\text{m}^2\text{K}$ , 0.81 % Solar heat gain coefficient (SHGC), 0.76 % Visible light transmittance (VT)) as well as a microalgae biowindow shading system. The FESDs possess different depth, length, and angle dimensions presented in Table 4 to contribute to daylight regulation. The material of static shadings is aluminum with  $237\text{W}/\text{mK}$  thermal conductivity [71],  $896 \text{ J}/\text{kgK}$  specific heat,  $2740 \text{ kg}/\text{m}^3$  density, and infrared emittance 0.25 [72].

The base model is examined in two types of semi-arid or steppe climates covering about 40 % of Iran's area based on the Köppen-Geiger climate classification. This climate type includes Hot semi-arid "BSh" (15.70 %) and Cold semi-arid "BSk" (23.69 %), whose representative cities in this study are Dezful and Shiraz, respectively. They are two well-known historical cities in Iran. Their climate data are presented in Table 3.

## 2.2. Simulation and objective functions

In the present study, three performance metrics, including Energy Use Intensity (EUI), Useful Daylight Illuminance (UDI), and Thermal Comfort Percentage (TCP) are selected to be optimized by investigating the optimum design options.

- **Energy Use Intensity (EUI):** The energy simulation examines the annual energy loads, which is a combination of Thermal energy use intensity (TEUI), including heating EUI ( $\text{EUI}_{\text{Heating}}$ ) and cooling EUI ( $\text{EUI}_{\text{Cooling}}$ ) as well as lighting EUI ( $\text{EUI}_{\text{Lighting}}$ ) and equipment EUI ( $\text{EUI}_{\text{Equipment}}$ ), which can be concluded by the following formulas:

$$\text{EUI}_{\text{Heating}} = \sum_{i=1}^{i=N_h} \text{EU}_{hi} / M \quad (1)$$

$$\text{EUI}_{\text{Cooling}} = \sum_{i=1}^{i=N_c} \text{EU}_{ci} / M \quad (2)$$

$$\text{EUI}_{\text{Thermal}} = \text{EUI}_{\text{Heating}} + \text{EUI}_{\text{Cooling}} \quad (3)$$

$$\text{EUI}_{\text{Lighting}} = \sum_{i=1}^{i=N_l} \text{EU}_{li} / M \quad (4)$$

$$\text{EUI}_{\text{Equipment}} = \sum_{i=1}^{i=N_e} \frac{\text{EU}_{ei}}{M} \quad (5)$$

Where  $\text{EU}_i$  (kWh) indicates hourly energy demand,  $N_h$ ,  $N_c$ ,  $N_l$ ,  $N_e$  indicate annual heating, cooling, lighting, and equipment hours, respectively.  $M$  is the floor area of the model. Hence, the overall EUI ( $\text{kWh}/\text{m}^2/\text{yr}$ ), which is the calculated energy types along with electrical equipment used within the building divided by gross floor area [73–75], can be calculated as:

$$\text{EUI} = \text{EUI}_{\text{Thermal}} + \text{EUI}_{\text{Lighting}} + \text{EUI}_{\text{Equipment}} \quad (6)$$

- **Useful Daylight Illuminance (UDI):** UDI is the unitless annual daylight performance metric proposed by Ref. [76] and defined as the ratio of time number of the studied points receiving enough daylight illuminances based on the specific ranges to the total number of operating hours. The range includes a lower threshold ( $\text{UDI}_{\text{underlit}}$ ), an upper threshold ( $\text{UDI}_{\text{overlit}}$ ), and an acceptable range as  $\text{UDI}_{\text{useful}}$  [77].

$$\left\{ \begin{array}{l} \text{UDI} = \frac{\sum_i (wf_i \cdot t_i)}{\sum_i t_i} \in [0, 1] \\ \text{UDI}_{\text{Overall}} \text{ with } wf_i = \begin{cases} 1 & \text{if } E_{\text{Daylight}} > E_{\text{Upper limit}} \\ 0 & \text{if } E_{\text{Daylight}} \leq E_{\text{Upper limit}} \end{cases} \\ \text{UDI}_{\text{Useful}} \text{ with } wf_i = \begin{cases} 1 & \text{if } E_{\text{Lower limit}} \leq E_{\text{Daylight}} \leq E_{\text{Upper limit}} \\ 0 & \text{if } E_{\text{Daylight}} < E_{\text{Lower limit}} \end{cases} \\ \text{UDI}_{\text{Underlit}} \text{ with } wf_i = \begin{cases} 1 & \text{if } E_{\text{Daylight}} < E_{\text{Lower limit}} \\ 0 & \text{if } E_{\text{Daylight}} \geq E_{\text{Lower limit}} \end{cases} \end{array} \right. \quad (7)$$

Where  $t_i$  indicates time fraction,  $E_{\text{Daylight}}$  (Lux) is the sole daylight, and  $wf_i$  is a weighting factor related to the  $E_{\text{Daylight}}$  value. According

to Brembilla and Mardaljevic [78], the UDI ranges for analysis can be calculated between 100 for non-sufficient, 100-300- for sufficient, 300 to 3000 for autonomous, and above 3000 for exceeded.

- **Thermal Comfort:** This building performance metric can be characterized as an individual perception of the thermal condition [79], and it is defined as a mind status indicating a person satisfaction with the thermal environment, which can be evaluated subjectively [80]. Two methods, including static and adaptive models are present to evaluate thermal comfort, while each one has advantages and disadvantages. The first method proposed by Fanger [81] is the basis for air-conditioned buildings with PMV and PPD, while the latter addresses naturally-ventilated ones. When PMV and PPD ignore the user's adaptation to the thermal environment and suffer from low accuracy [82], adaptive thermal comfort (ATC) utilized by Ref. [83] focuses on the occupants' active reaction to adjust themselves to the environment by using the relationship between mean monthly outdoor air temperature (OAT) and indoor operative temperature (IOT). To measure the indoor comfort temperature ( $T_{co}$ ) according to the reference mean outdoor air temperature ( $T_{ref}$ ), the following formula can be applied [29]:

$$T_{co} = 0.31 \times T_{ref} + 17.8^\circ C \quad (8)$$

$T_{ref}$  is calculated based on the time (7–30 days) before the day in question. In the present study, annual TCP (%) is used, which is examined by the formula [84]:

$$TCP = \sum_{i=1}^q \frac{wf_i}{q} \times 100 \% \quad (9)$$

$$\text{With } wf_i = \begin{cases} 1 & \text{if } T_{lo} \leq T \leq T_{Up} \\ 0 & \text{if } T < T_{lo} \vee > T_{Up} \end{cases} \quad (10)$$

Where  $T$  and  $q$  indicate IOT and total hour, respectively, while  $T_{Up}$  and  $T_{Lo}$  are upper and lower air temperatures calculated as:

$$T_{Up} = 0.31 \times T_{ref} + 20.3^\circ C \quad (11)$$

$$T_{Lo} = 0.31 \times T_{ref} + 15.3^\circ C \quad (12)$$

### 2.3. Optimization

The optimal value of an optimization problem, which is searching for maximum/minimum values or applying one/multi-objective, can be searched through the optimization process [85]. Though applying MOO based on Building Performance Simulation (BPS), complicated building performance trade-offs can be investigated regarding the impact of the changing design variables on the studied objectives and finding the optimal design solutions [86]. The MOO problem can be defined mathematically as:

$$\text{Min / Max } f_1(x), f_2(x), \dots, f_n(x) \quad (13)$$

Subject to:  $x \in U$ .

Where  $x$ ,  $n$ ,  $U$ , and  $f(x)$  are MOO solutions, number of objective functions, feasible set, and objective function, respectively. Also, min and max refer to the combined object operation.

There are two methods through which complex mathematical processes are not required to address the MOO problem, including Pareto and scalarization. The Pareto method can be applied when the solutions and performance metrics are presented as Pareto optimal front (POF) and are different tared-off solutions based on the concept of dominated and non-dominate solutions, which can be mathematically presented as follows [87]:

$$f_{1,opt} = \min f_1(x) \quad (14)$$

$$f_{2,opt} = \min f_2(x)$$

- 
- 

$$f_{n,opt} = \min f_n(x)$$

Furthermore, the scalarization is based on the scalar function included in the fitness function [88] based on the following formula [89]:

$$F(x) = w_1 f_1(x) + w_2 f_2(x) + \dots + w_M f_M(x) \quad (15)$$

Where  $w$  is the weighting coefficient.

In the present study, the MOO technique is applied to find optimum design options considering minimum EUI, maximum UDI, and TCP as follows:

$$F_1(x) = \min(\text{EUI}) \quad (16)$$

$$F_2(x) = \max(\text{UDI})$$

$$F_3(x) = \max(\text{TCP})$$

In the first step of optimization, Octopus a Grasshopper plugin for MOO was used, which is developed based on the Strength Pareto Evolutionary Algorithm (SPEA- II) and the Hypervolume Estimation Algorithm (HypE). It possesses attributes like trade-off finding, alteration of the objective metrics during the searching process, searching for trade-offs, forcing diversity of solutions, visualization, and result exploration [90]. The SPEA- II is a powerful and efficient multi-objective evolution algorithm, that performs similarly to the widely applied NSGA-II [91]. Besides, HypE as a hypervolume-based multi-objective algorithm employs Monte Carlo simulation to estimate the exact hypervolume values [92]. The hypervolume calculates the criterion space volume dominated by the points of the Pareto front, which make a bounded space and can illustrate the hypervolume indicator along with a reference point. The hypervolume indicator can be presented mathematically as [93]:

$$I_H(\text{PF}, \mathbf{r}) = \lambda \left( \bigcup_{s \in \text{PF}} \text{Space}(s, \mathbf{r}) \right)$$

$$\mathbf{r} = (r_1, r_2, \dots, r_c) \in \mathbb{R}^C \quad (17)$$

$$\text{Space}(s, \mathbf{r}) = \{ \mathbf{v} \in \mathbb{R}^C \mid \mathbf{r} \prec \mathbf{v} \leq \mathbf{s} \}$$

Where  $\mathbf{r}$  is a reference point,  $\text{Space}(s, \mathbf{r})$  is criterion space,  $\mathbf{v}$  is criterion vector,  $\lambda$  is Lebesgue measure and

$$\text{PF} \in \mathbb{R}^C \text{ is indicated as } I_H(\text{PF}).$$

There are different methods to select the optimum solution among different Pareto-fronts such as technique for order of preference by similarity to ideal solution (TOPSIS) [94,95], linear programming technique for multidimensional analysis of preference (LINMAP) [96], faire un choix adequate (FUCA) [97], preference ranking organization method for enrichment of evaluations II (PROMETHEE II) [98], clustering and closest to the ideal point [99], and fuzzy membership function [100]. Among the mentioned methods, TOPSIS is known as the common selection method based on the ideal solution [101].

In the second step of MOO, to select the absolute optimum solution within the non-dominated solutions, the TOPSIS method adopted by Refs. [94,102,103] was used by applying an MS Excel-based program. The principle of the method is that the selected design solution should be the nearest to the positive ideal or ideal solution while it should be the farthest from the negative ideal point. To use the TOPSIS method, the following steps should be taken [95,103,104].

(1) Normalize the decision matrix (m rows & n column) by:

$$F_{ij} = f_{ij} / \sqrt{\sum_{i=1}^m f_{ij}^2} \quad (18)$$

(2) Calculate the weighted normalized decision matrix by:

$$v_{ij} = w_j \times F_{ij} \quad (19)$$

Where  $w_j$  and  $v_{ij}$  are the weight of the  $i$ th attribute/criterion and weighted normalized value, respectively.

(3) Define the positive ( $A^+$ ) and negative ( $A^-$ ) ideal solutions:

$$A^+ = \{v_1^+, \dots, v_n^+\} = \{(\text{Max}_i(v_{ij}) \mid j \in J), (\text{Min}_i(v_{ij}) \mid j \in J')\} \quad (20)$$

$$A^- = \{v_1^-, \dots, v_n^-\} = \{(\text{Min}_i(v_{ij}) \mid j \in J), (\text{Max}_i(v_{ij}) \mid j \in J')\} \quad (21)$$

Where  $J$  indicates the set of maximization  $s$  and  $J'$  shows the set of minimization objectives. The best values regarding maximization and minimization objectives are defined as the largest and smallest values. In contrast the worst values for maximization and minimization objectives are the smallest and largest values within the column of the objective matrix, respectively.

(4) Measure the Euclidean distance  $S_{i+}$  and  $S_{i-}$  from positive and negative ideal solutions for each alternative:

$$S_{i+} = \sqrt{\sum_{j=1}^n (v_{ij} - v_j^+)^2} \quad i = 1, 2, 3, \dots, m \quad (22)$$

$$S_{i-} = \sqrt{\sum_{j=1}^n (v_{ij} - v_j^-)^2} \quad i = 1, 2, 3, \dots, m \tag{23}$$

(5) Measure the relative closeness of each optimal solution to the ideal solution:

$$C_i = S_{i-} / S_{i-} + S_{i+} \tag{24}$$

Because  $S_{i+} \geq 0$ , and  $S_{i-} \geq 0$ , so  $C_i \in [0, 1]$ .

Accordingly, defined Pareto solutions derived from the MOO process with the best EUI, UDI, and TCP for both studied climate zones were recommended using the mentioned method.

- Design variables

The algorithm was determined based on the window characteristics and the shading systems. In the present study, the design parameters are WWR, dimension, and angle of FESDs, including vertical louver (V-louver), horizontal louver (H-louver), overhang, overhang and fin (OF) as well as bioshading system. Value ranges for each shading variable are presented in Table 4. To evaluate a wide range of shading features, shading depth is changed at 0.05 m and for the angle at 5-degree intervals. WWR ranges also change at 10–90 % at 5 % intervals.

The simulation of ABBS is based on [61] (Fig. 3), who evaluated different thermal characteristics of microalgae windows through experimentation and examined its thermal performances when integrated with building façade by simulation research methods. U-factor, VT, and SHGC of an ABBS, including *Chlorella vulgaris* species are presented in Table 4. Since the culture density of microalgae potentially changes due to cell growth, light penetration differs based on various culture densities, resulting in different thermal features. Accordingly, eight densities were defined [61] from 20 % to 100 % to evaluate the impact of microalgae concentration on the determined objective metrics and investigate the optimum culture density considering daylight and energy performance of the school building. Also, the U-factor was considered 4.9 W/m<sup>2</sup>K during a year, despite the small changes in summer and winter [61]. It is noteworthy to state that although PBR density changes based on the growth rate of the microalgae, the algae concentration in

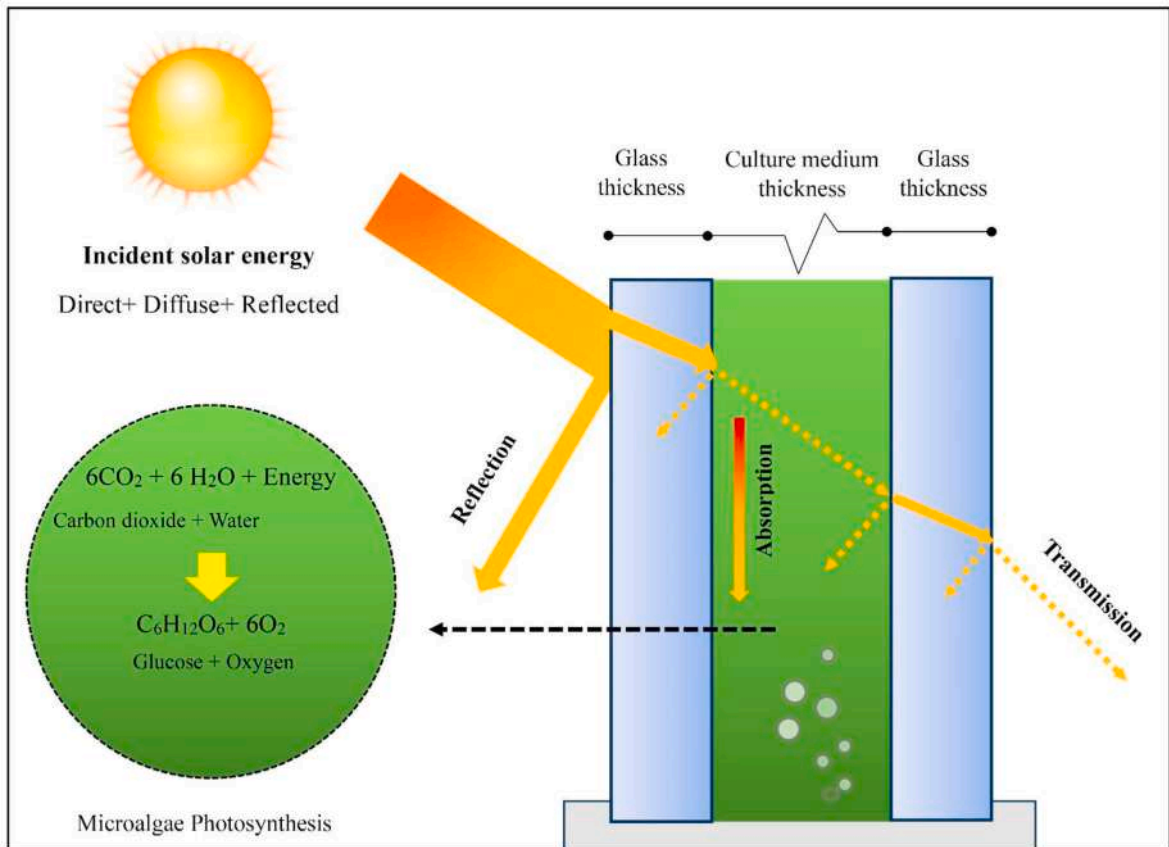


Fig. 3. Schematic section of microalgae window and the photosynthesis process (Authors based on [61,105,106]).

**Table 5**  
Genomes with best TCP, best UDI, and best EUI among Pareto frontiers.

			WWR (%)	Depth (m)	Angle(°)	Density	TCP (%)	UDI (%)	EUI (kWh/m <sup>2</sup> /yr)	Heating (kWh/m <sup>2</sup> /yr)	Cooling (kWh/m <sup>2</sup> /yr)	Lighting (kWh/m <sup>2</sup> /yr)	
<b>Dezful</b>													
North	H-Louver	B*.TCP	85	0.50	60		<b>90.41</b>	76.41	187.00	3.37	129.61	13.05	
		B.UDI	90	0.35	-15		82.86	<b>96.57</b>	193.95	3.62	139.24	10.12	
		B.EUI	30	0.15	65		88.06	62.08	<b>164.93</b>	1.84	110.12	12.00	
	V-Louver	B.TCP	55	0.55	-50		<b>88.98</b>	69.76	174.45	2.48	118.95	12.05	
		B.UDI	0.85	0.15	-30		80.98	<b>92.64</b>	190.18	3.57	135.12	10.52	
		B.EUI	20	0.6	0		88.05	25.68	<b>163.29</b>	1.64	106.15	14.53	
	Overhang	B.TCP/B.EUI	15	0.7	40		<b>74.32</b>	37.68	<b>169.4</b>	0.35	111.76	16.32	
		B.UDI	55	0.9	50		61.07	<b>86.08</b>	187.1	0.1	135.57	10.47	
		B.TCP	55	1.00	SA***: 85, TA***:85		<b>88.72</b>	74.18	175.30	2.48	120.585	11.26	
	OF	B.UDI	65	0.70	SA:10, TA: 25		83.23	<b>94.61</b>	181.45	2.827	127.282	10.367	
		B.EUI	20	0.30	SA: 40, TA:5		86.08	58.45	<b>162.70</b>	1.637	106.944	13.145	
		ABBS	B.TCP	25			40	<b>85.82</b>	80.64	164.44	1.79	109.87	11.81
			B.UDI	50			50	83.63	<b>93.11</b>	176.39	2.43	122.52	10.47
			B.EUI	20			30	85.67	67.48	<b>163.54</b>	1.64	107.84	13.10
		Base model					84.23	92.51	173.85	2.282	120.04	10.565	
	South	H-Louver	B.TCP	75	0.70	55		<b>85.71</b>	52.85	194.89	2.431	130.506	20.982
			B.UDI	65	0.70	0		63.35	<b>90.32</b>	179.51	0.942	127.48	10.119
			B.EUI	30	1.00	-20		68.83	62.58	<b>165.43</b>	0.397	113.244	10.813
V-Louver		B.TCP	10	0.60	20		<b>75.98</b>	15.96	169.64	0.397	110.863	17.411	
		B.UDI	50	0.45	-10		56.55	<b>82.20</b>	189.14	0.149	137.55	10.466	
		B.EUI	10	0.45	0		73.82	21.30	<b>165.92</b>	0.397	109.673	14.881	
Overhang		B.TCP	10	0.40	30		<b>72.93</b>	30.03	169.64	0.248	111.161	17.262	
		B.UDI	45	0.90	20		62.18	<b>85.93</b>	180.80	0.099	129.117	10.615	
		B.EUI	15	0.50	-20		67.63	63.47	<b>166.52</b>	0.149	113.542	11.855	
OF		B.TCP	10	0.95	SA: 65, TA:5		77.49	14.15	170.98	0.397	109.97	19.643	
		B.UDI	50	0.90	SA: 25, TA:50		64.89	<b>86.21</b>	179.56	0.149	127.778	10.665	
		B.EUI	15	0.95	SA:0, TA: 25		69.86	55.50	<b>163.49</b>	0.198	110.169	12.153	
ABBS		B.TCP/B.EUI	10			60	<b>68.96</b>	44.30	<b>168.90</b>	0.149	114.335	13.442	
		B.UDI	30			40	58.38	81.26	187.80	0.05	136.359	10.417	
		Base model					51.57	78.51	205.7	0.05	154.514	10.169	
<b>Shiraz</b>													
North		H-Louver	B.TCP	55	0.85	65		<b>85.25</b>	2.39	127.58	12.153	51.538	22.917
			B.UDI	80	0.25	30		71.44	<b>97.54</b>	121.18	14.831	55.06	10.317
	B.EUI		30	0.15	60		81.20	69.07	<b>109.47</b>	11.458	45.188	11.855	
	V-Louver	B.TCP	80	0.60	-80		<b>86.28</b>	64.25	120.39	15.129	53.571	10.714	
		B.UDI	80	0.60	10		77.56	<b>96.45</b>	119.89	15.129	53.026	10.764	
		B.EUI	35	0.50	0		82.62	74.52	<b>109.33</b>	11.954	45.337	11.062	
	Overhang	B.TCP	15	0.45	75		<b>78.94</b>	26.26	113.89	9.921	44.544	18.452	
		B.UDI	55	0.50	40		72.55	<b>95.24</b>	116.42	13.194	51.24	11.012	
		B.EUI	20	0.30	-80		77.73	72.20	<b>108.93</b>	10.714	44.345	12.897	
	OF	B.TCP	30	0.75	SA: 30, TA:85		<b>82.28</b>	50.19	111.06	11.26	45.238	13.591	
		B.UDI	85	0.90	SA: 10, TA:70		73.93	<b>95.87</b>	122.02	15.377	55.258	10.417	
		B.EUI	20	0.35	SA:15, TA:85		79.47	45.45	<b>108.09</b>	10.714	43.502	12.897	
	ABBS	B.TCP	15			30	<b>78.03</b>	50.77	110.16	10.21	43.84	15.12	
		B.UDI	50			100	72.23	<b>94.96</b>	115.62	13.09	51.09	10.46	
		B.EUI	20			30	77.79	71.88	<b>108.87</b>	10.71	44.29	12.89	
	Base model					73.12	94.7	114.13	12.748	49.901	10.516		
	South	H-Louver	B.TCP	75	0.45	60		<b>75.92</b>	86.26	116.87	12.401	52.282	11.21

(continued on next page)

Table 5 (continued)

		WWR (%)	Depth (m)	Angle(°)	Density	TCP (%)	UDI (%)	EUI (kWh/m <sup>2</sup> /yr)	Heating (kWh/m <sup>2</sup> /yr)	Cooling (kWh/m <sup>2</sup> /yr)	Lighting (kWh/m <sup>2</sup> /yr)
V-Louver	B.UDI	75	0.50	30		70.11	<b>93.41</b>	116.67	11.657	53.075	10.962
	B.EUI	40	0.20	65		52.68	81.90	<b>105.26</b>	4.613	49.157	10.516
	B.TCP	85	0.85	80		<b>80.71</b>	18.56	128.87	12.649	57.54	17.708
Overhang	B.UDI	0.35	0.25	0		38.18	<b>84.61</b>	106.65	2.679	52.53	10.466
	B.EUI	25	0.45	10		49.37	66.77	<b>104.96</b>	4.911	47.966	11.111
	B.TCP	15	0.95	60		<b>69.49</b>	18.77	112.00	6.399	46.032	18.601
OF	B.UDI	55	0.90	45		40.40	<b>89.17</b>	108.63	2.381	54.762	10.516
	B.EUI	20	0.25	-15		45.89	80.76	<b>103.22</b>	2.629	48.611	11.012
	B.TCP	10	0.85	A:50,TA:70		<b>69.28</b>	2.11	116.27	6.101	46.081	23.115
ABBS	B.UDI	50	1	SA: 25, TA:40		47.282	<b>90.42</b>	106.696	4.514	50.446	10.764
	B.EUI	15	0.4	SA: 45,TA: 15		54.70	62.41	<b>102.53</b>	4.018	45.536	12.004
	B.TCP	10			20	<b>54.46</b>	45.40	105.31	3.968	46.825	13.542
Base model	B.UDI	30			40	37.33	<b>84.74</b>	108.98	1.24	56.25	10.516
	B.EUI	15			40	47.61	69.85	<b>104.37</b>	3.075	48.562	11.756
						30.68	81.15	116.56	0.595	64.732	10.268

\*B: Best \*\*SA: Side angle \*\*\*TA: Top angle.

NB: The value of the best TCP, best UDI and best EUI for each shading type are bold to be clearer.

the closed system PBR can be potentially regulated and kept constant when needed.

To achieve the research objective, 20 MOO processes were conducted for five studied shading systems within two selected climate zones. Considering one orientation, there are 11,951 total possible design options for V-louver, H-louver, and overhang, separately. Also, for OF and bioshading system number of design options are 442,187, and 136, respectively. The total numbers for all shading systems become doubled (956,352) considering both north- and south-facing windows for each city. Accordingly, the whole number of design solutions for both Shiraz and Dezful is 1912704, separately. Thermal comfort, daylight and energy performance objectives of the optimum solutions were compared with those of the base model.

### 3. Results and discussion

The results of daylight, energy, and thermal comfort performance metrics through the MOO process are presented in this section. First, the results of Pareto solutions for north- and south-oriented windows considering the best EUI, TCP, and UDI in Dezful and Shiraz are analyzed and compared with the related performance metric in the base model (Table 5). Then, the studied performance objectives of the absolute optimum genomes selected by the TOPSIS method for each window orientation are analyzed compared to that of the base model (Table 6). Last, the interaction between the design variables and energy, daylight, and thermal performance is investigated through sensitivity analysis.

The performance metrics of the north- and south windows of the base models in Dezful, including TCP, UDI, and EUI are 84.23 %,92.51 %,173.85 kWh/m<sup>2</sup>/yr, and 51.57 %,78.51 %, 205.70 kWh/m<sup>2</sup>/yr, respectively and sequentially. The results indicate that considering all objective metrics, the north-oriented window surpasses the south one. In Shiraz, the results of the studied objective of the base model are the same as Dezful. In Shiraz, TCP, UDI, and EUI of the north-oriented model are 73.12 %, 94.70 %, 114.13 kWh/m<sup>2</sup>/yr, while that of the south-oriented model are 30.68 %,81.15 %,116.56 kWh/m<sup>2</sup>/yr, respectively, which still demonstrate the priority of the north window in both BSK and BSH climates. Accordingly, investigating the performance of applying different shading devices is important to enhance energy, daylight, and thermal comfort indices of a school building in the studied cities.

#### 3.1. Analysis of the pareto-frontier solutions

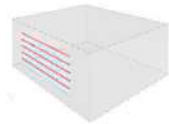
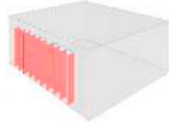
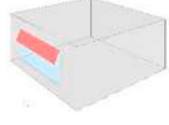
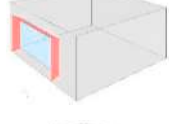

The results of this section are presented in Table 5. Also, to evaluate and visualize the design solutions and to illustrate Pareto fronts more obviously, the TT toolbox, Colibri [90] and Design Explorer [107] were used to illustrates the relationship between studied design variables and the performance metrics presented in the Supplementary material.

##### 3.1.1. Dezful

- *North orientation:* In the north-oriented model, the best daylight and thermal comfort performance are dedicated to H-louver with high WWR by 7.38 % TCP and 4.38 % UDI improvement. However, the most considerable energy performance is for the OF-integrated model with 6.41 % EUI reduction, followed by V-louver by 6.07 %, ABBS by 5.93 %, H-louver by 5.13 % and overhang by 2.55 %. Meanwhile, the worst performance metrics belong to the overhang with 11.77 % TCP, and 6.95 % UDI level reduction, with only 2.55 % EUI improvement compared to the other studied systems. The range of applied WWR is 15 and 55 % for this system. Besides, ABBS could provide 1.89 % and 0.64 % TCP and UDI improvement, respectively. Also, the culture density for the PBR system is between 30 % and 50 %. In general, except for the overhang, all the other applied shading systems enhance thermal comfort and daylight level. Considering energy performance, all five shadings potentially improve energy efficiency in school buildings.

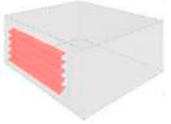
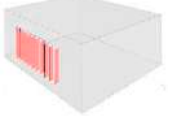
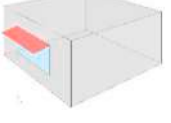

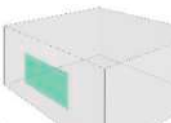


**Table 6**  
Parameters and objectives of the absolute optimum genomes.

	WWR (%)	Depth (m)	Angle (°)	Density	TCP (%)	UDI (%)	EUI kWh/m2/yr	Heating	Cooling	Lighting	Fitness Function	View	
Dezful North	H-Louver	40	0.10	25		85.96	90.22	169.59	2.13	115.77	10.71	0.82072	
	V-Louver	55	0.45	0		<b>87.68</b>	<b>91.79</b>	174.45	2.48	119.49	11.51	0.86303	
	Overhang	35	0.75	65		65.72	80.02	175.69	0.15	123.66	10.91	0.7832	
	OF	35	70	SA*: 20 TA**: 25		86.19	88.61	<b>167.26</b>	1.984	113.095	11.21	0.8124	
	ABBS	35			50	85.34	90.02	168.8	2.03	114.88	10.91	0.8024	
	Base model					84.23	92.51	173.85	2.282	120.04	10.565		

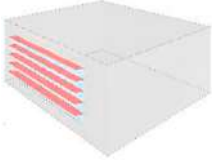
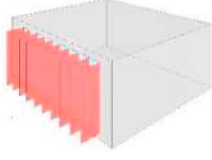
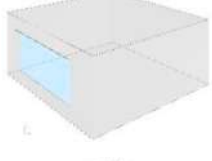
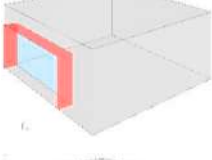
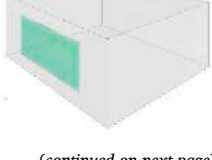
(continued on next page)

Table 6 (continued)

	WWR (%)	Depth (m)	Angle (°)	Density	TCP (%)	UDI (%)	EUI kWh/m2/yr	Heating	Cooling	Lighting	Fitness Function	View	
South	H-Louver	45	0.45	30		<b>79.31</b>	<b>81.15</b>	<i>182.99</i>	1.042	121.577	19.395	0.7982	
	V-Louver	30	0.30	-10		62.65	79.25	176.64	0.149	124.157	11.359	0.7964	
	Overhang	25	1.00	10		69.05	80.05	170.44	0.198	116.22	13.046	0.8648	
	OF	25	1.00	SA:40 TA: 10		69.1	77.49	<b>166.62</b>	0.198	114.484	10.962	0.8388	
	ABBS	20			30	63.17	77.52	176.59	0.102	124.603	10.913	0.7741	
Shiraz	Base model					51.57	78.51	205.7	0.05	154.514	10.169		

(continued on next page)

Table 6 (continued)

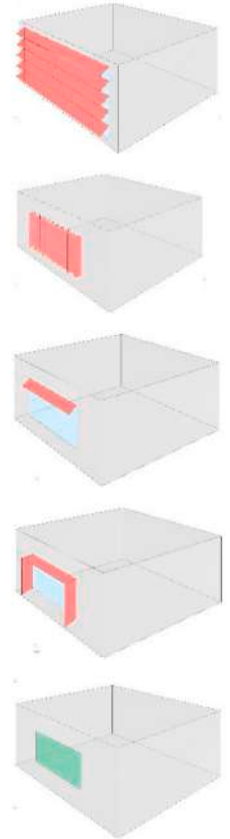
	WWR (%)	Depth (m)	Angle (°)	Density	TCP (%)	UDI (%)	EUI kWh/m2/yr	Heating	Cooling	Lighting	Fitness Function	View	
North	H-Louver	45	0.45	-10		79.5	92.68	112.95	12.351	48.81	10.813	0.9198	
	V-Louver	70	0.95	0		<b>84.59</b>	<b>94.37</b>	<i>117.71</i>	14.286	51.091	11.359	0.8719	
	Overhang	35	0.40	-35		75.37	92.89	<b>111.11</b>	11.954	47.371	10.813	0.933	
	OF	40	0.65	SA:5 TA: 5		75.92	93.23	111.46	12.202	47.421	10.863	0.8526	
	ABBS	35			40	75.1	92.67	111.409	12.004	47.619	10.813	0.9038	

(continued on next page)

Table 6 (continued)

	WWR (%)	Depth (m)	Angle (°)	Density	TCP (%)	UDI (%)	EUI kWh/m2/yr	Heating	Cooling	Lighting	Fitness Function	View
South	Base model					73.12	94.7	114.13	12.748	49.901	10.516	
	H-Louver	75	0.50	30		<b>70.11</b>	<b>93.41</b>	<i>116.67</i>	11.657	53.075	10.962	0.7208
	V-Louver	30	0.35	30		50.43	73.25	106.1	4.117	49.901	11.111	0.6902
	Overhang	30	0.45	40		44.55	85.84	105.01	2.728	50.198	11.111	0.7281
	OF	25	0.75	SA: 30 TA: 5		53.3	80.62	<b>102.579</b>	4.415	46.131	11.062	0.8096
	ABBS	20			30	43.06	80.21	105.31	2.331	50.992	11.012	0.7901
	Base model					30.68	81.15	116.56	0.595	64.732	10.268	

\*SA: Side angle \*\*TA: Top angle.

NB: The best value of each objective for each orientation is **bold**, and the worst value is *Italic* to be more explicit.

- **South orientation:** In the south-oriented model H-louvers surpasses the other shading systems in terms of thermal and daylight performances. It improves TCP by 66.20 % followed by OF (50.26 %), V-louvers (47.33 %), overhang (41.41 %), and ABBS (33.72 %). WWR for all the cases is 10 % except for the H-louvers with 75 % WWR. Also, by 15.04 % UDI improvement, H-louvers stands at the first rank, while OF by 9.80 %, overhang by 9.45 %, V-louvers by 4.70 %, and ABBS by 3.50 % stands at the second, third, fourth and fifth ranks, respectively. Furthermore, the same as the north-oriented model, the OF-installed classroom with 15 % WWR has the highest energy improvement of 20.52 % followed by H-louvers, V-louvers, and overhang by 19.57 %, 19.33 %, 19.04 %, respectively and sequentially. Meanwhile, ABBS (10 % WWR) by 17.89 % still has the lowest contribution to the model's energy efficiency.

Overall, regarding only the best performance metrics, the overhang for the north and bioshading system for the south window has the worth performance in terms of all objective metrics compared to the other studied shadings in the hot stepped climate of Dezful. However, the H-louvers is superior to the other systems regarding daylight and thermal comfort indices, while OF plays a key role in energy use reduction of the school building compared to the other shading devices.

3.1.2. Shiraz

- **North orientation:** The results of the north-and south-oriented facades are almost similar in Shiraz. In both building aspects, the best TCP, UDI, and EUI are dedicated to V-louvers, H-louvers, and OF models. Besides, the less favorable shading options for both TCP and UDI are ABBS (15 % and 50 % WWR) for north orientation and ABBS (10 % WWR) and V-louvers (35 % WWR) for south orientation. Considering EUI, the less optimum shading is H-louvers in two studied orientations. In the north, the greatest TCP improvement value is dedicated to the V-louvers by 17.99 %, followed by the H-louvers (16.58 %), OF (12.52 %), overhang (7.95 %), and ABBS (6.71 %). Moreover, UDI has been improved by 2.99 %, 1.84 %, 1.23 %, 0.57 %, and 0.27 % for H-louvers, V-louvers, OF, overhang, and microalgae window, respectively.

- **South orientation:** The lowest thermal comfort level is for south-oriented classroom in Shiraz by 30.68 % TCP. However, applying any kind of the studied shading systems can considerably enhance daylight metric. Accordingly, the highest thermal performance is dedicated to the V-louvers-installed model (85 % WWR) by 163.07 %, and the lowest still belongs to ABBS (10 % WWR) by 54.46 % TCP improvement. Meanwhile, H-louvers by 147.45 %, overhang by 126.49 %, and OF by 125.81 % have second, third, and fourth ranks in terms of TCP enhancement, respectively. H-louvers with 93.41 % UDI can improve the index by 15.10 % as the most suitable shading system, in comparison V-louvers with 84.61 % UDI can improve daylight metrics by 4.26 %, as the least favorable

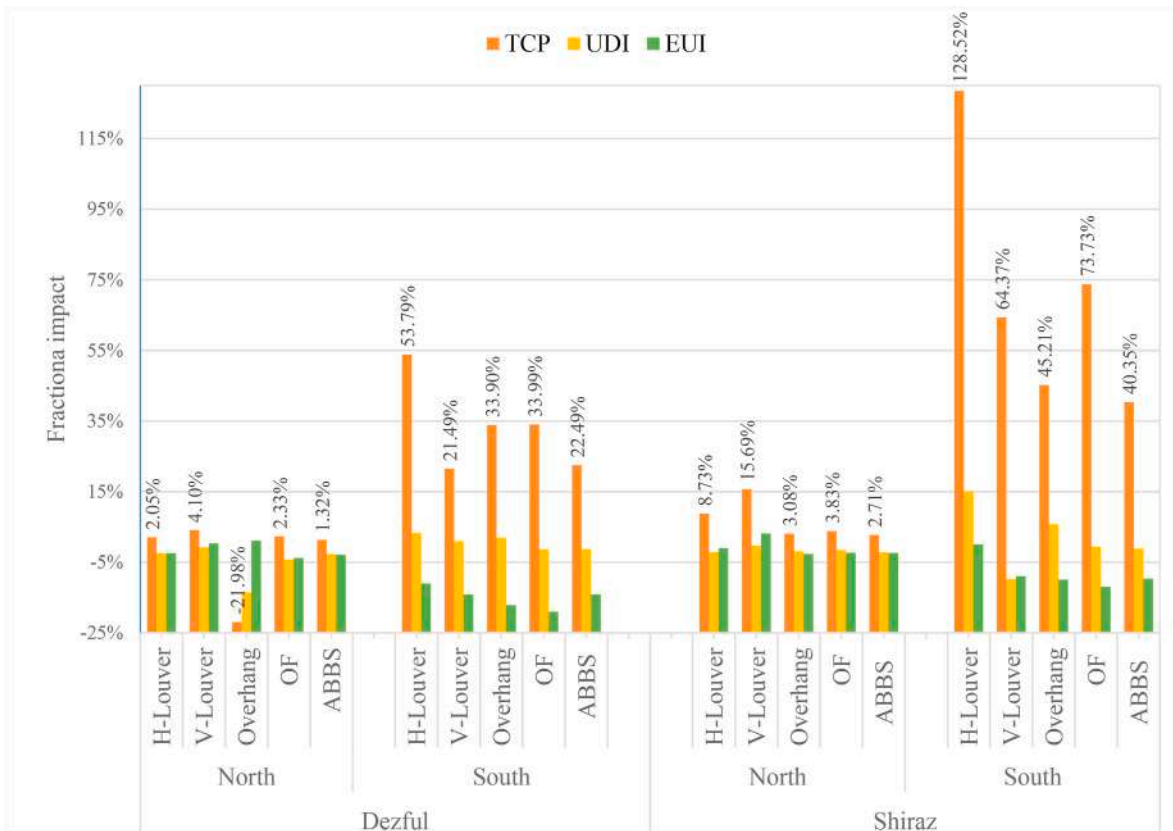


Fig. 4. Fractional impact of thermal comfort, daylight, and energy use differences of the absolute genomes compared to the base case.

option to control daylight level. In terms of EUI, again OF has the highest energy use reduction by 12.06 %, while the lowest energy efficiency is for the H-louver-installed model with an EUI value of 105.26 kWh/m<sup>2</sup>/yr resulting in 9.69 % energy efficiency.

Generally, in both BSk and BSh climates, the best genomes with the highest UDI values are for H-louver with high WWR and low angle, and the best solutions considering EUI are OF-installed models with 15 % or 20 % WWR. Besides, the best performance to control daylight metric is dedicated to the south-oriented V-louver with 15.10 % UDI improvement in the BSk climate. The best energy performance of also occurs in the south-oriented window in the hot climate of Dezful by 20.52 % EUI reduction compared to the base model.

### 3.2. The absolute optimum genomes

Results of the selected absolute optimum genomes based on the TOPSIS method (Section 2.3) are summarized and discussed in the following sections. Table 6 shows the value of the performance metrics and the shading/window characteristics. Fig. 4 illustrates the fractional impact of the shadings on each objective and Fig. 5 illustrates TCP/UDI of the absolute optimum solutions. Fig. 6, also shows comparisons of the performance metrics of the base model, absolute optimum solutions and Pareto-fronts concerning the best single objective.

#### 3.2.1. Dezful

- **North orientation:** In the north-oriented window model, the V-louver provides the highest thermal comfort with 87.68 % TCP, which enhances the index by 4.10 % compared to the base model. Accordingly, all the shading systems contribute to improving TCP except for the overhang, which reduces thermal comfort by 21.98 %. Although the base model surpasses all the design options regarding daylight, since all the shadings reduce the UDI level, overhang again has the worst performance by 13.50 % daylight index reduction. Meanwhile, V-louver stands at the first rank by 0.78 % UDI reduction. Considering EUI, except for the overhang by 1.05 % and V-louver by 0.34 % EUI enhancements, the other shadings improve energy saving. The best design option for energy efficiency is OF by 3.79 % contribution to EUI reduction. Compared to the other systems, the studied bioshading stands at the fourth rank in thermal comfort, with 1.32 % TCP improvement, the third rank in daylight metrics with 2.69 % UDI reduction, and at the second rank in energy saving by 2.90 % EUI improvement.

**South orientation:** In this orientation, all the shading devices enhance thermal comfort contrary to the north window, with greater improvement in TCP level. The highest TCP enhancement is dedicated to the H-louver at 53.79 %, while the lowest is for V-louver at 21.98 %. Considering daylight, again H-louver contributes the most to UDI improvement by 3.36 % and OF the least by 1.29 % UDI reduction. Like the north façade, the OF by 18.99 % EUI decrease has the greatest contribution to energy efficiency, while H-louver by 11.04 % plays the worst performance. The role of any shading system in energy efficiency is more acceptable in the south façade than the north in hot stepped climate of Dezful. This can be attributed to the high sun radiation through the south-oriented window, which the studied shading systems can control. ABBS stands at the fourth rank considering thermal comfort and daylight metrics and the third rank regarding energy efficiency by 22.49 %, -1.26 %, and -14.15 % fractional impact, respectively.

Generally, in Dezful, the V-louver provides the highest TCP and UDI levels, and OF contributes to the energy efficiency of the building more significantly than the other systems in both orientations. Also, overhang has the most undesirable performance considering any objectives in the north orientation. Besides, all south-faced FESDs have greater depths and are integrated with lower WWR compared to the north orientation due to the high solar radiation in the south aspect. However, only the H-louver can be deployed on the more extended window by 45 % WWR compared to the H-louver in the north by 40 % WWR.

#### 3.2.2. Shiraz

**North orientation:** The same as the hot climate of Dezful, V-louver has the most noticeable role in TCP improvement by 15.68 % and the most negligible role in UDI reduction by 0.34 % in Shiraz. At the same time, the worst performance metrics are dedicated to the ABBS. However, V-louver is the only shading device, which does not provide energy efficiency for the building owing to enhancing EUI value by 3.13 %. Nevertheless, energy use reduction is achieved using any shading system except for the V-louver. Also, the highest EUI value reduction is dedicated to the overhang by 2.64 %.

**South orientation:** Thermal comfort and daylight performance of the H-louver stands at the highest level among other systems like the south-oriented model in Dezful. It enhances TCP and UDI indices by 128.52 % and 15.10 %, respectively. Also, the least contribution to thermal and daylight metrics are for ABBS by 40.35%TCP improvement and V-louver by 9.73 % UDI reduction. Except for the H-louver, which enhances EUI by 0.09 %, all the shadings provide energy savings for the classroom. The highest energy efficiency belongs to OF with 11.99 %, and the lowest is for V-louver with 8.97 % EUI reduction. With the last rank in TCP, the fourth in UDI, and the third in EUI, ABBS does not surpass the other shadings, considering any performance metrics.

Overall, in the BSk climate, the V-louver in the north and H-louver in the south have the most potential to improve the daylight and thermal performance of a school building. Besides, overhang and OF perform the most considerable role in energy saving in the north and south, respectively. Except for the H-louver, WWR in the south façade integrated with any shading systems is reduced compared to the north. This can highlight the potential of the H-louver in controlling solar radiation to improve the studied objective in the south-oriented window. Also, the depth of all FESDs is smaller in the north than south, which can be attributed to the lower sun radiation. However, the only shading, with more extensive northern depth, is V-louver. WWR of the bioshading system in north and south orientations in BSk and BSh climates are the same equal to 35 % and 20 %, respectively. Besides, the microalgae culture density in the south orientation in both climates is 30 %, while in the north, it is 50 % and 40 % in Dezful and Shiraz, in order.

Generally, the results can be summarized and discussed as follows.



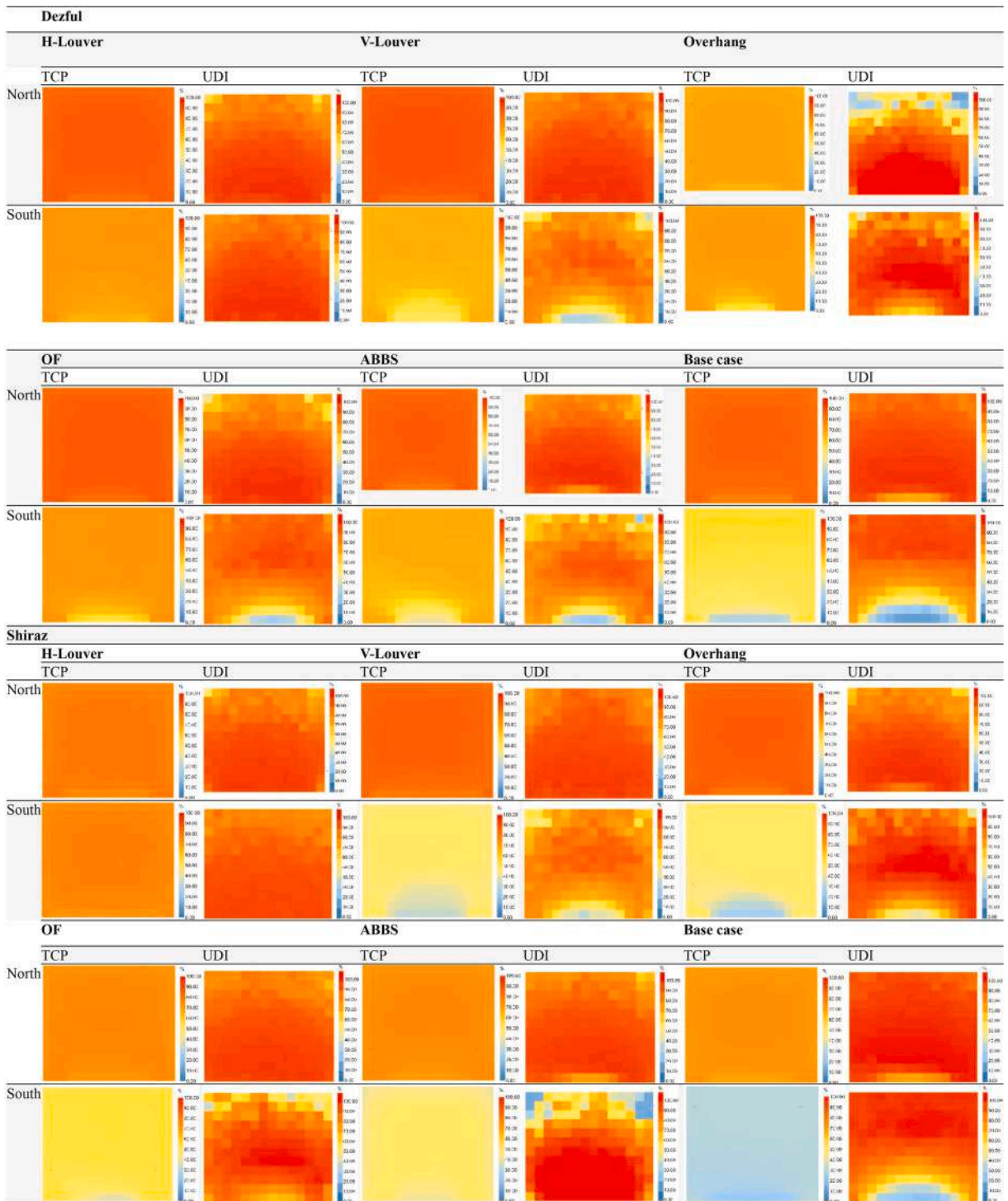


Fig. 5. TCP and UDI of the absolute optimum solutions.

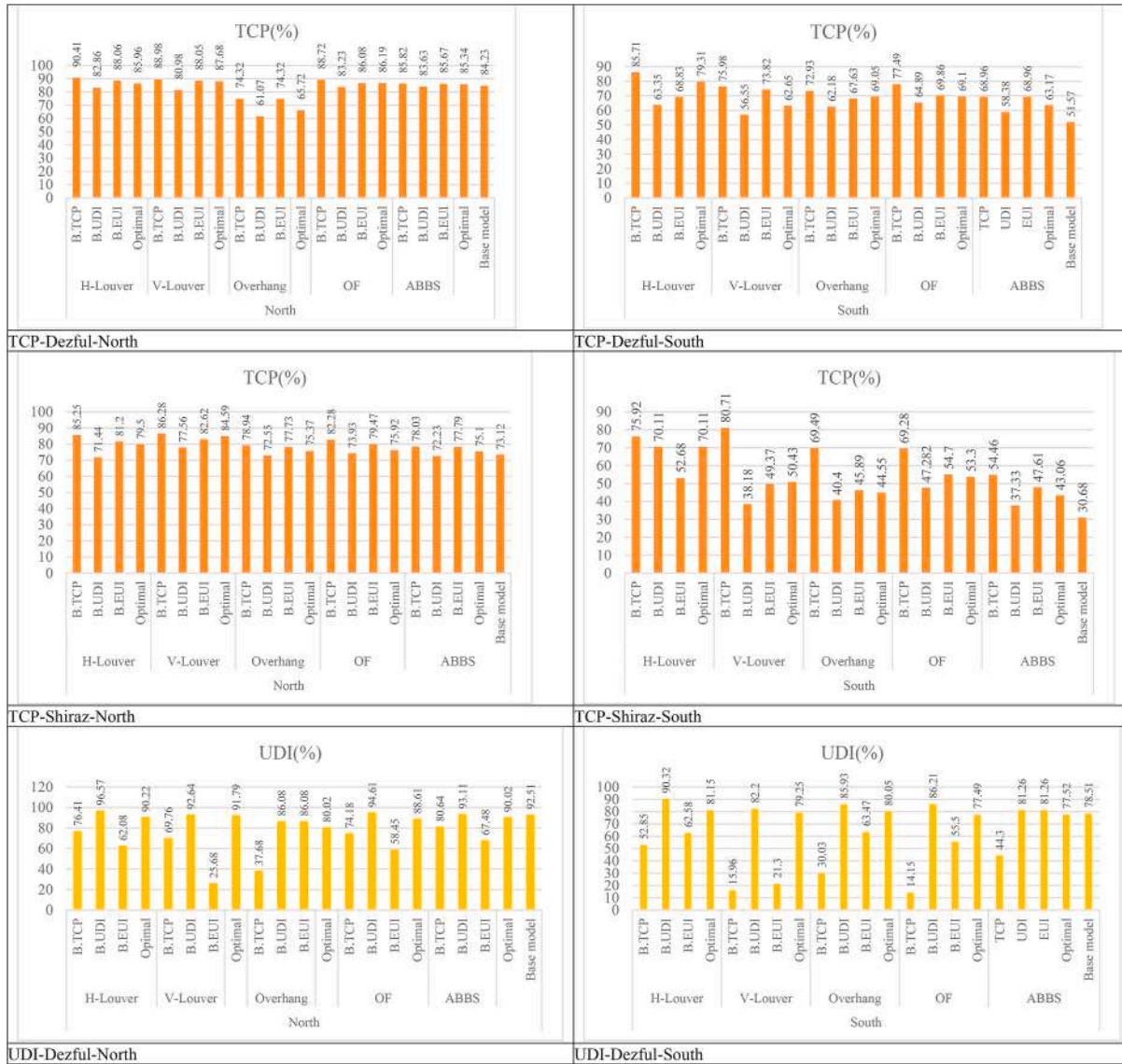


Fig. 6. Comparisons of the performance metrics of the base model, absolute optimum genomes and pareto-front solutions concerning each best single objectives (Best TCP, UDI, and EUI).

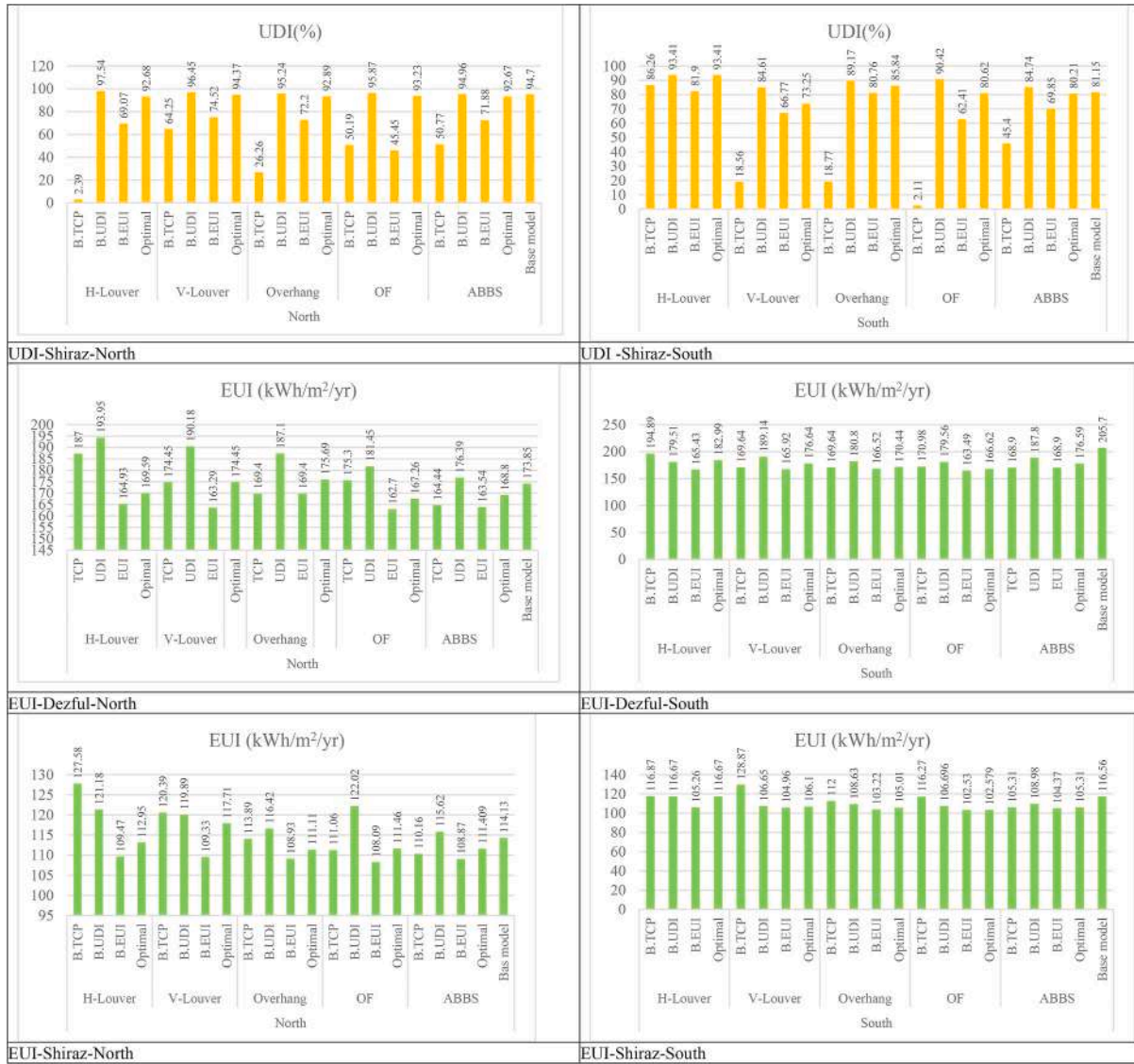


Fig. 6. (continued).

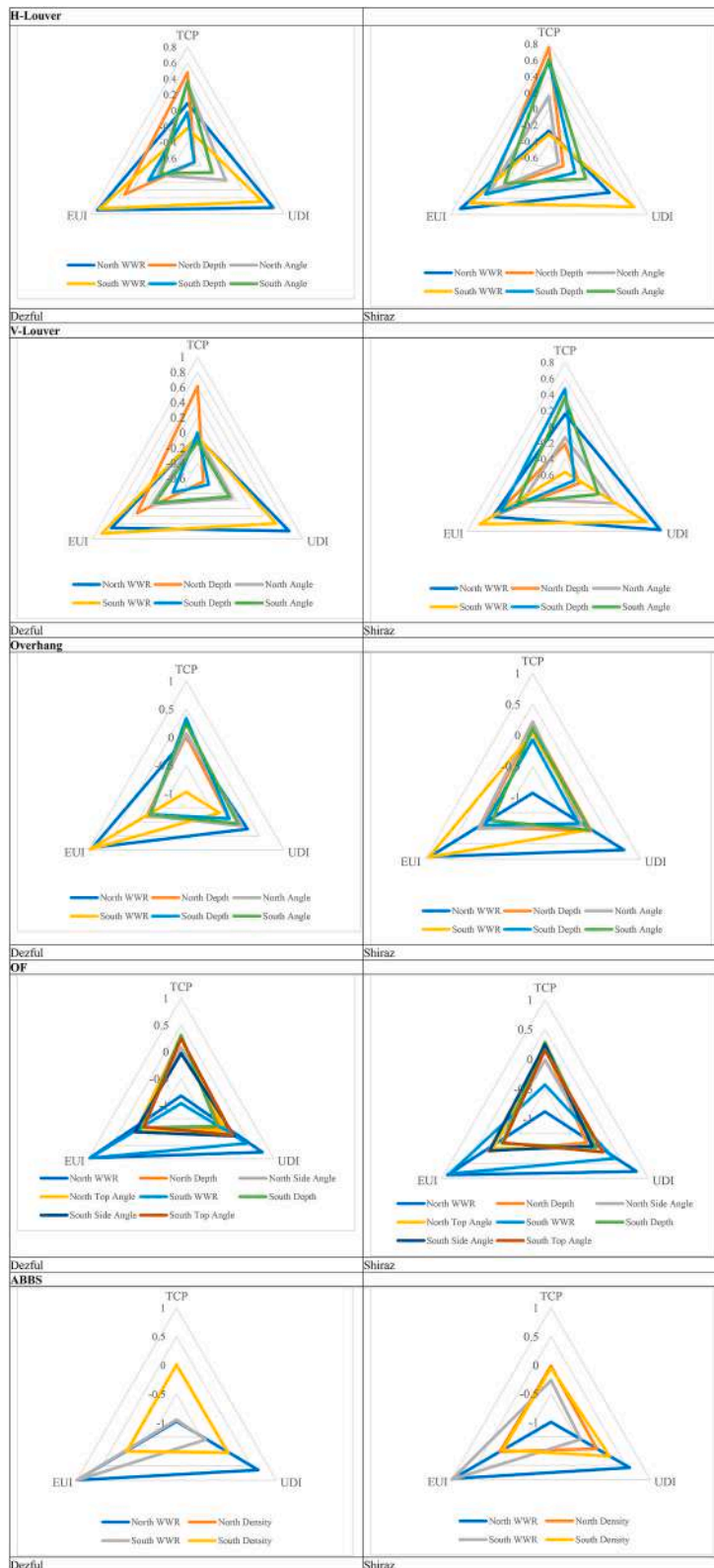


Fig. 7. SRC for design variables including shading characteristics and window size on TCP, UDI and EUI.



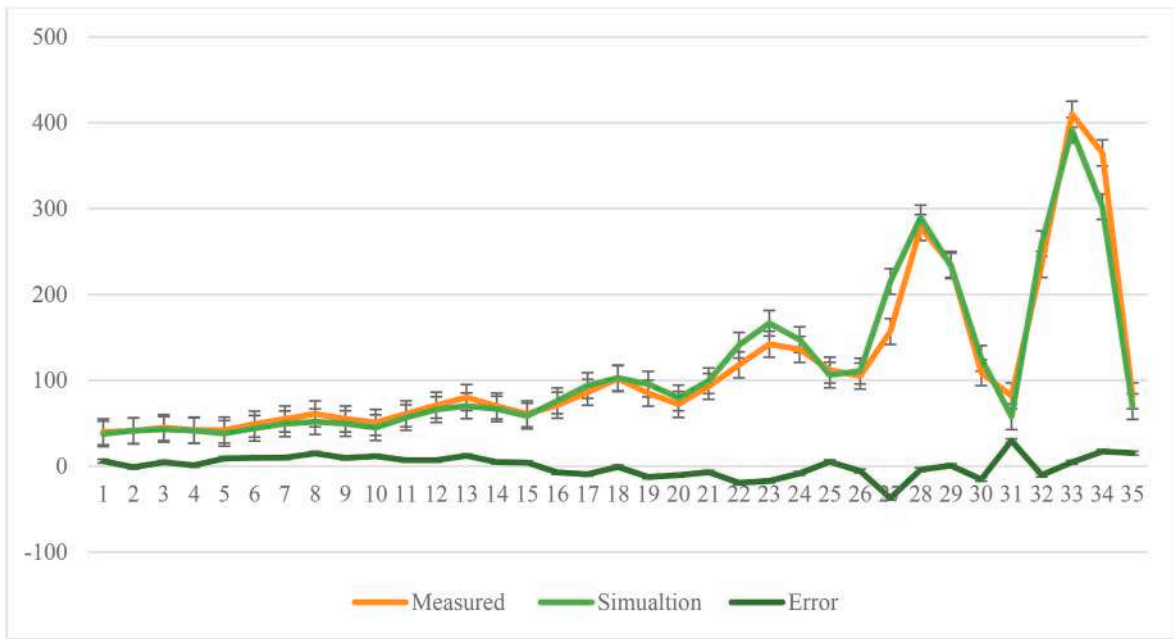


Fig. 8. In-situ measurements and simulation results based on point-by-point illuminance level.

- Thermal and daylight performances of all the studied shading systems are more effective in the south-oriented classroom in the BSk climate compared to the other orientations and locations. At the same time, the worst performance happens in the north orientation in Dezful. The only exception is the V-louver installed model, which has the lowest daylight performance by 9.73 % UDI reduction. Accordingly, the least TCP improvement is devoted to the ABBS by 40.35 %, which is still considerably higher than the performance of the other shadings in the north orientation and BSh climate.
- The highest energy improvement is assigned to the shadings deployed on the south-oriented façade in the hot climate of Dezful, where the cooling load is greater than the BSk climate. Furthermore, OF plays the most noticeable role in providing energy efficiency for all the cases studied compared to the other shading strategies, except for the north-oriented model in Shiraz, where overhang has the highest energy use reduction.

Considering bioshading strategy, ABBS has no superiority over the other shading systems in terms of the studied objective metrics. It is also not recommended to be applied in the north orientation in Shiraz, considering its weak performance in enhancing thermal and daylight indices. However, it always contributes to improving the energy efficiency of the educational building in both climate zones.

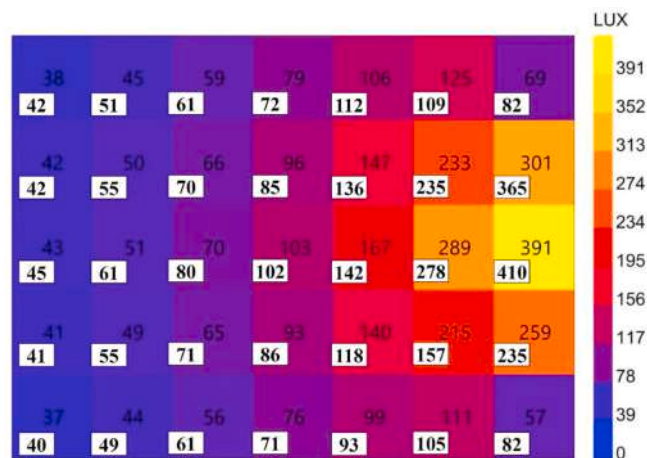


Fig. 9. Validation of the simulated model against in-situ measurement.

### 3.3. Sensitivity analysis

Sensitivity analysis is a validated tool [108] applied to investigate the most dominant and contributing variables to the objectives and can define some interactivity within the model [109]. As a common method in building energy studies [110], sensitivity analysis is applied in this research to investigate the significance of the design variables, including shading features and WWR on the thermal comfort, daylight, and energy performance of a classroom in stepped climate zones. Hence, multiple linear regression (MLR) as a common method of sensitivity analysis is applied, which uses Standardized Regression Coefficients (SRC) and Unstandardized Regression Coefficient (USRC) to analyze the relationship between variables and the objectives. The value of SRC expresses the significance of the relationship between the variables and the objectives, and positive/negative signs show their direct/indirect relationship. SRC calculation is based on the following formula:

$$SRC_j = \beta_j \sqrt{\frac{Var(X_j)}{Var(Y)}} \quad (25)$$

Where  $X_j$  and  $Y$  are variable and the output respectively, and  $\beta_j$  is linear regression coefficient related to  $X_j$ . Besides,  $SRC_j^2$  indicates the share of variance (Fig. 7). The results can be expressed as:

- *H-louwer*: The depth of the H-louwer has the highest positive impact on TCP and UDI in the north- and south-oriented model in Dezful, respectively. However, in Shiraz, its depth has the greatest positive impact on only TCP with the lowest positive effect on EUI in north orientation. The angle of the H-louwer also plays a less effective role in UDI and EUI metrics in the north-oriented façade and has the greatest impact on TCP in the south model in Dezful and Shiraz.
- *V-louwer*: The depth of the V-louwer-installed model, as the most influential parameter, positively impacts TCP considering the north orientation in Dezful and Shiraz. However, its angle is regarded as the least effective variable on all the studied objective functions in the north model in Dezful and Shiraz's north and south model.
- *Overhang*: Overhang depth has a positive impact on TCP and a negative relationship with UDI and EUI in Dezful. Besides, in Shiraz, it negatively affects energy performance in the north and all performance metrics in the south orientation. Overhang depth and TCP relationship is always positive, except for the south model in Shiraz. It is also considerable that the overhang angle is the least influential parameter on all the studied objectives in the south model in Dezful.
- *OF*: While OF depth positively influences the thermal comfort of all the design options, it always negatively impacts daylight and energy performance, considering both studied climate zones and orientations. The only exception is the positive impact on EUI in Shiraz' north façade. Side and top angles are also the least dominant variables on TCP and UDI, respectively, in Dezful' north and south orientations compared to the other variables.

*ABBS*: In all studied models, the concentration of the bioshading system has less influence on thermal, daylight, and energy metrics compared to WWR. The microalga density has a positive impact on thermal and daylight and a negative impact on energy indices in Dezful. Hence, the denser culture medium results in higher TCP and UDI and lower EUI values. However, in the north-oriented model in Shiraz, density negatively impacts TCP and UDI and positively influences EUI. Though, in the south orientation, it has a negative relationship with TCP and EUI and a positive correlation with UDI.

## 4. Validation

Honeybee v.0.0.64 [111], v.0.0.65, v.1.4.0 [112], v.0.0.69 [62], and HoneybeePlus v.0.0.04 [113] plugins have been already evaluated by previous studies. In the present study, to evaluate the accuracy of the simulation, the results of the daylight simulation by Honeybee of LBT v.1.6.0 based on Daysim and Radiance engines are compared with a real building. The in-situ measurement was carried out by Refs. [113,114] based on comparing the point-by-point illuminance results. In this study, the error of average illuminance result is below 3 %, which is in accordance with the previous studies [113,115]. The difference between the simulation model and the experimental data can be attributed to the data of the weather files and the real condition of the field measurement [31], and the restriction of the software to estimation, calculation, and simulation of the building thermal behavior [116]. Accordingly, the results of this paper are presented based on a validated model. Figs. 8 and 9 illustrate the results of the simulation and measurement.

## 5. Conclusion and future research

Through developing a MOO framework and sensitivity analysis, the present study bridges the knowledge gap in applying shading strategies to address the environmental performance of a school building by making a comparison between a novel bioshading system and common shading devices in stepped climate zones. To achieve this goal the microalgae culture system as an avant-garde bioshading strategy is compared with vertical/horizontal louvers, overhang, and combination of overhang and fins integrated with the north and south school facade to improve daylight, thermal comfort, and energy performance metrics. MOO framework can examine the studied objective metrics of the school building while proposing optimized design solutions for each orientation and climate zone. Furthermore, sensitivity analysis is applied to investigate the relationship between the variables of interest, including shading characteristics (dimension, angle, density) and WWR, and the design objectives. The simulator engine Honeybee was also validated by evaluating its results' accuracy by comparing it with the in-filed measurement. The results of this research indicate that.



- Microalgae bioshading does not stand at the first rank to enhance all the objective metrics compared to the other shading systems in none of the examined climates. Its best thermal comfort performance is demonstrated in the south-oriented window in Dezful by 4.035 % TCP improvement. Considering daylight, all the absolute optimum design solutions with bioshading slightly reduce UDI level by 1.15 %–2.69 %. Besides, the best energy performance of the school facade integrated with ABBS is dedicated to the south orientation in Dezful by 14.15 % EUI reduction. Results also present that the WWR of solutions with ABBS is almost the lowest compared to the other systems in the south orientation of both climates. This can be attributed to the lower sun radiation control of the bioshading compared to the static shadings.
- All the studied shading devices greatly improve thermal comfort when integrated with the southern aspect of the school building in the stepped climate. The most noticeable thermal performance refers to the H-louwer-installed south-oriented façade in Shiraz by 128.52 % TCP augmentation. It also dedicates the first rank in boosting daylight metric by 15.10 % within all the studied shading systems. Except for the north V-louwer in Shiraz/Dezful, the south H-louwer in Shiraz, and the north overhang in Dezful, all the other design solutions contribute to improving the energy efficiency of the school building. However, shadings' role in controlling energy consumption is more considerable in the south orientation in stepped climate. Nevertheless, applying any shading system has more favorable impact on energy saving in the hot climate of Dezful than Shiraz, due to the higher need for sun radiation control. OF-integrated southern façade in Dezful shows the greatest energy improvement by 18.99 % EUI reduction, while the V-louwer on the north-oriented façade in Shiraz increases energy consumption by 3.13 %.

WWR in all absolute optimum design options negatively impacts thermal comfort except for the positive relationship in Dezful' north H-louwer as well as Shiraz' north V-louwer, and south overhang. On the contrary, sensitivity analysis demonstrates the positive impact of WWR on daylight metric. The only negative relationships are dedicated to south overhang and ABBS in Dezful and south ABBS in Shiraz. Considering the energy metric, the greater the WWR, the higher the energy consumption in all design options. It is also demonstrated that WWR has the highest SRC on EUI compared to the other metrics. The only exceptions are the north V-louwer in Dezful and Shiraz as well as north ABBS and north/south H-louwer in Shiraz. In general, microalgae bioshading system has advantages and disadvantages compared to FESDs, considering the studied objective metrics. However, integrating microalgae PBR as newly-emerged façade technology has further noticeable advantages like CO<sub>2</sub> sequestration, O<sub>2</sub>, and biofuel production as significant added values to the building, while other shading systems lack such environmental potentials. Future research should consider not only the thermal, daylight, and energy metrics of the ABBS system in other climate zones, but also its noticeable potential to improve buildings' environmental impact compared to and in integration with other shading systems like smart glasses, photovoltaic panel shading, adaptable shadings, etc. Furthermore, further studies need to be conducted on the other objective metrics including more daylight factors like sDA, ASE, Daylight Factor (DF), visual comfort indexes, cost, life cycle impact etc. Studies can also focus on more design variables such as shading/wall materials, different HVAC systems, building geometry, proportions, and façade type. Besides, the MOO framework can be developed for more building types in different geographical locations.

### CRediT authorship contribution statement

**Maryam Talaei:** Writing – review & editing, Writing – original draft, Validation, Supervision, Software, Methodology, Investigation, Formal analysis, Data curation, Conceptualization. **Hamed Sangin:** Visualization, Validation, Software, Resources, Investigation, Data curation.

### Declaration of competing interest

The authors declare that they have no known competing financial interests or personal relationships that could have appeared to influence the work reported in this paper

### Data availability

Data will be made available on request.

### Appendix A. Supplementary data

Supplementary data to this article can be found online at <https://doi.org/10.1016/j.job.2024.109435>.

### References

- [1] Z. Wang, W. Wang, Y. Zhang, J. Song, L. Zhu, Research on energy-saving design strategies of libraries in severe cold regions: taking a university in Xinjiang as an example, *Energy Rep.* 7 (2021) 1101–1113, <https://doi.org/10.1016/j.egy.2021.09.160>.
- [2] T. Méndez Echenagucia, A. Capozzoli, Y. Cascone, M. Sassone, The early design stage of a building envelope: multi-objective search through heating, cooling and lighting energy performance analysis, *Appl. Energy* 154 (2015) 577–591, <https://doi.org/10.1016/j.apenergy.2015.04.090>.
- [3] K. Lakhdari, L. Sriti, B. Painter, Parametric optimization of daylight, thermal and energy performance of middle school classrooms, case of hot and dry regions, *Build. Environ.* 204 (2021) 108173, <https://doi.org/10.1016/j.buildenv.2021.108173>.
- [4] R. Loonen, J. Rico-Martinez, F. Favoino, M. Brzezicki, C. Menezes, G. La Ferla, L. Aelenei, Design for façade adaptability: towards a unified and systematic characterization, *10th Conf. Adv. Build. Ski.* (2015) 1284–1294.

- [5] R.A. Mangkuto, M.D. Koerniawan, S.R. Apriliyanthi, I.H. Lubis Atthallah, J.L.M. Hensen, B. Paramita, Design optimisation of fixed and adaptive shading devices on four façade orientations of a high-rise office building in the tropics, *Buildings* 12 (2022), <https://doi.org/10.3390/buildings12010025>.
- [6] Y. Zou, S. Lou, D. Xia, I.Y.F. Lun, J. Yin, Multi-objective building design optimization considering the effects of long-term climate change, *J. Build. Eng.* 44 (2021) 102904, <https://doi.org/10.1016/j.jobte.2021.102904>.
- [7] P. Pilechiha, M. Mahdavinjad, F. Pour Rahimian, P. Carnemolla, S. Seyedzadeh, Multi-objective optimisation framework for designing office windows: quality of view, daylight and energy efficiency, *Appl. Energy* 261 (2020) 114356, <https://doi.org/10.1016/j.apenergy.2019.114356>.
- [8] A. Ciardiello, F. Rosso, J. Dell'Olmo, V. Ciancio, M. Ferrero, F. Salata, Multi-objective approach to the optimization of shape and envelope in building energy design, *Appl. Energy* 280 (2020) 115984, <https://doi.org/10.1016/j.apenergy.2020.115984>.
- [9] Y. Fang, X. Luo, J. Lu, A review of research on the impact of the classroom physical environment on schoolchildren's health, *J. Build. Eng.* 65 (2023) 105430, <https://doi.org/10.1016/j.jobte.2022.105430>.
- [10] P.M. Bluysen, Health, comfort and performance of children in classrooms - new directions for research, *Indoor Built Environ.* 26 (2017) 1040–1050, <https://doi.org/10.1177/1420326X16661866>.
- [11] B.J. Alkhatatbeh, Y. Kurdi, S. Asadi, Enhancing learning environments: exploring optimal classroom design connected to double-loaded corridors across the U.S. climate zones, *Energy Build.* 298 (2023) 113562, <https://doi.org/10.1016/j.enbuild.2023.113562>.
- [12] A. Wirz-Justice, D.J. Skene, M. Münch, The relevance of daylight for humans, *Biochem. Pharmacol.* 191 (2021) 114304, <https://doi.org/10.1016/j.bcp.2020.114304>.
- [13] R. Küller, C. Lindsten, Health and behavior of children in classrooms with and without windows, *J. Environ. Psychol.* 12 (1992) 305–317, [https://doi.org/10.1016/S0272-4944\(05\)80079-9](https://doi.org/10.1016/S0272-4944(05)80079-9).
- [14] K.P. Wright, A.W. McHill, B.R. Birks, B.R. Griffin, T. Rusterholz, E.D. Chinoy, Entrainment of the human circadian clock to the natural light-dark cycle, *Curr. Biol.* 23 (2013) 1554–1558, <https://doi.org/10.1016/j.cub.2013.06.039>.
- [15] P. Wargocki, J.A. Porras-Salazar, S. Contreras-Espinoza, The relationship between classroom temperature and children's performance in school, *Build. Environ.* 157 (2019) 197–204, <https://doi.org/10.1016/j.buildenv.2019.04.046>.
- [16] D. Wang, Y. Xu, Y. Liu, Y. Wang, J. Jiang, X. Wang, J. Liu, Experimental investigation of the effect of indoor air temperature on students' learning performance under the summer conditions in China, *Build. Environ.* 140 (2018) 140–152, <https://doi.org/10.1016/j.buildenv.2018.05.022>.
- [17] W.K. Alhuwayil, F.A. Almazaid, M. Abdul Mujeeb, Energy performance of passive shading and thermal insulation in multistory hotel building under different outdoor climates and geographic locations, *Case Stud. Therm. Eng.* 45 (2023) 102940, <https://doi.org/10.1016/j.csite.2023.102940>.
- [18] I. Elzeyadi, The impacts of dynamic façade shading typologies on building energy performance and occupant's multi-comfort, *Architect. Sci. Rev.* 60 (2017) 316–324, <https://doi.org/10.1080/00038628.2017.1337558>.
- [19] M. Rabani, H. Bayera Madessa, N. Nord, Achieving zero-energy building performance with thermal and visual comfort enhancement through optimization of fenestration, envelope, shading device, and energy supply system, *Sustain. Energy Technol. Assessments* 44 (2021) 101020, <https://doi.org/10.1016/j.seta.2021.101020>.
- [20] S. Wen, X. Hu, G. Hua, P. Xue, D. Lai, Comparing the performance of four shading strategies based on a multi-objective genetic algorithm: a case study in a university library, *J. Build. Eng.* 63 (2023) 105532, <https://doi.org/10.1016/j.jobte.2022.105532>.
- [21] A. Kiritmat, O. Krejcar, B. Ekici, M. Fatih Tasgetiren, Multi-objective energy and daylight optimization of amorphous shading devices in buildings, *Sol. Energy* 185 (2019) 100–111, <https://doi.org/10.1016/j.solener.2019.04.048>.
- [22] J. Zhao, Y. Du, Multi-objective optimization design for windows and shading configuration considering energy consumption and thermal comfort: a case study for office building in different climatic regions of China, *Sol. Energy* 206 (2020) 997–1017, <https://doi.org/10.1016/j.solener.2020.05.090>.
- [23] K.W. Chen, P. Janssen, A. Schlueter, Multi-objective optimisation of building form, envelope and cooling system for improved building energy performance, *Autom. Construct.* 94 (2018) 449–457, <https://doi.org/10.1016/j.autcon.2018.07.002>.
- [24] Y. Xu, G. Zhang, C. Yan, G. Wang, Y. Jiang, K. Zhao, A two-stage multi-objective optimization method for envelope and energy generation systems of primary and secondary school teaching buildings in China, *Build. Environ.* 204 (2021) 108142, <https://doi.org/10.1016/j.buildenv.2021.108142>.
- [25] Y. Xu, C. Yan, Y. Pan, K. Zhao, M. Li, F. Zhu, Y. Jiang, A three-stage optimization method for the classroom envelope in primary and secondary schools in China, *J. Build. Eng.* 52 (2022) 104487, <https://doi.org/10.1016/j.jobte.2022.104487>.
- [26] E. Noorzai, P. Bakmohammadi, M.A. Garmaroudi, Optimizing daylight, energy and occupant comfort performance of classrooms with photovoltaic integrated vertical shading devices, *Architect. Eng. Des. Manag.* 19 (2023) 394–418, <https://doi.org/10.1080/17452007.2022.2080173>.
- [27] J.H. Park, B.Y. Yun, S.J. Chang, S. Wi, J. Jeon, S. Kim, Impact of a passive retrofit shading system on educational building to improve thermal comfort and energy consumption, *Energy Build.* 216 (2020), <https://doi.org/10.1016/j.enbuild.2020.109930>.
- [28] Y. Xu, C. Yan, D. Wang, J. Li, J. Shi, Z. Lu, Q. Lu, Y. Jiang, Coordinated optimal design of school building envelope and energy system, *Sol. Energy* 244 (2022) 19–30, <https://doi.org/10.1016/j.solener.2022.08.035>.
- [29] A. Zhang, R. Bokel, A. van den Dobbelssteen, Y. Sun, Q. Huang, Q. Zhang, Optimization of thermal and daylight performance of school buildings based on a multi-objective genetic algorithm in the cold climate of China, *Energy Build.* 139 (2017) 371–384, <https://doi.org/10.1016/j.enbuild.2017.01.048>.
- [30] Y. Xu, C. Yan, G. Wang, J. Shi, K. Sheng, J. Li, Y. Jiang, Optimization research on energy-saving and life-cycle decarbonization retrofitting of existing school buildings: a case study of a school in Nanjing, *Sol. Energy* 254 (2023) 54–66, <https://doi.org/10.1016/j.solener.2023.03.006>.
- [31] F. Dokhanian, M. Mohajerani, H. Estaji, M. Nikravan, Shading design optimization in a semi-arid region: considering energy consumption, greenhouse gas emissions, and cost, *J. Clean. Prod.* 428 (2023) 139293, <https://doi.org/10.1016/j.jclepro.2023.139293>.
- [32] F. De Luca, A. Sepúlveda, T. Varjas, Multi-performance optimization of static shading devices for glare, daylight, view and energy consideration, *Build. Environ.* 217 (2022) 109110, <https://doi.org/10.1016/j.buildenv.2022.109110>.
- [33] F.M. Baba, H. Ge, R. Zmeureanu, L. Leon Wang, Optimizing overheating, lighting, and heating energy performances in Canadian school for climate change adaptation: sensitivity analysis and multi-objective optimization methodology, *Build. Environ.* 237 (2023), <https://doi.org/10.1016/j.buildenv.2023.110336>.
- [34] Y. Wang, W. Yang, Q. Wang, Multi-objective parametric optimization of the composite external shading for the classroom based on lighting, energy consumption, and visual comfort, *Energy Build.* 275 (2022) 112441, <https://doi.org/10.1016/j.enbuild.2022.112441>.
- [35] Q. Gao, Y. Yang, Q. Wang, An integrated simulation method for PVSS parametric design using multi-objective optimization, *Front. Archit. Res.* 11 (2022) 509–526, <https://doi.org/10.1016/j.foar.2021.11.003>.
- [36] A. Kuru, P. Oldfield, S. Bonser, F. Fiorito, Performance prediction of biomimetic adaptive building skins: integrating multifunctionality through a novel simulation framework, *Sol. Energy* 224 (2021) 253–270, <https://doi.org/10.1016/j.solener.2021.06.012>.
- [37] Y.J. Grobman, I.G. Capeluto, G. Austern, External shading in buildings: comparative analysis of daylighting performance in static and kinetic operation scenarios, *Architect. Sci. Rev.* 60 (2017) 126–136, <https://doi.org/10.1080/00038628.2016.1266991>.
- [38] A. Tabadkani, A. Roetzel, H. Xian, A. Tsangrassoulis, S. Attia, Analysis of the Impact of Automatic Shading Control Scenarios on Occupant's Comfort and Energy Load, 2021, p. 294.
- [39] A. Ganji Kheybari, M. Alwalidi, C. Hepf, T. Auer, S. Hoffmann, A multi-objective evaluation for envelope refurbishments with electrochromic glazing, *Results Eng* 14 (2022) 100417, <https://doi.org/10.1016/j.rineng.2022.100417>.
- [40] W. Feng, L. Zou, G. Gao, G. Wu, J. Shen, W. Li, Gasochromic smart window: optical and thermal properties, energy simulation and feasibility analysis, *Sol. Energy Mater. Sol. Cells* 144 (2016) 316–323, <https://doi.org/10.1016/j.solmat.2015.09.029>.
- [41] L.Y.L. Wu, Q. Zhao, H. Huang, R.J. Lim, Sol-gel based photochromic coating for solar responsive smart window, *Surf. Coating Technol.* 320 (2017) 601–607, <https://doi.org/10.1016/j.surfcoat.2016.10.074>.
- [42] M. Casini, Energy-generating glazing, in: *Smart Build.*, Woodhead Publishing, 2016, pp. 327–353, <https://doi.org/10.1016/b978-0-08-100635-1.00010-1>.
- [43] F. Ahmadi, S. Wilkinson, H. Rezaeizadeh, S. Keawsawasvong, Q. Najafi, A. Masoumi, Energy efficient glazing: a comparison of microalgae photobioreactor and Iranian Orosi window designs, *Build. Environ.* 233 (2022) 109942, <https://doi.org/10.1016/j.buildenv.2022.109942>.

- [44] A. Khani, M. Khakzand, M. Faizi, Multi-objective optimization for energy consumption, visual and thermal comfort performance of educational building (case study: qeshm Island, Iran), *Sustain. Energy Technol. Assessments* 54 (2022) 102872, <https://doi.org/10.1016/j.seta.2022.102872>.
- [45] B.J. Alkhatatbeh, Y. Kurdi, S. Asadi, Multi-objective optimization of classrooms' daylight performance and energy use in U.S. Climate zones, *Energy Build.* (2023) 113468, <https://doi.org/10.1016/j.enbuild.2023.113468>.
- [46] P. Bakmohammadi, E. Noorzai, Optimization of the design of the primary school classrooms in terms of energy and daylight performance considering occupants' thermal and visual comfort, *Energy Rep.* 6 (2020) 1590–1607, <https://doi.org/10.1016/j.egy.2020.06.008>.
- [47] S. Nateghi, J. Kaczmarczyk, Multi-objective optimization of window opening and thermostat control for enhanced indoor environment quality and energy efficiency in contrasting climates, *J. Build. Eng.* 78 (2023) 107617, <https://doi.org/10.1016/j.jobe.2023.107617>.
- [48] N. Ziaee, R. Vakilinezhad, Multi-objective optimization of daylight performance and thermal comfort in classrooms with light-shelves: case studies in Tehran and Sari, Iran, *Energy Build.* 254 (2022) 111590, <https://doi.org/10.1016/j.enbuild.2021.111590>.
- [49] J. Pruvost, B. Le Gouic, O. Lepine, J. Legrand, F. Le Borgne, Microalgae culture in building-integrated photobioreactors: biomass production modelling and energetic analysis, *Chem. Eng. J.* 284 (2016) 850–861, <https://doi.org/10.1016/j.cej.2015.08.118>.
- [50] E.S. Umdu, I. Kahraman, N. Yildirim, L. Bilir, Optimization of microalgae panel bioreactor thermal transmission property for building façade applications, *Energy Build.* 175 (2018) 113–120, <https://doi.org/10.1016/j.enbuild.2018.07.027>.
- [51] J. González-Martín, N.J.R. Kraakman, C. Pérez, R. Lebrero, R. Muñoz, A state-of-the-art review on indoor air pollution and strategies for indoor air pollution control, *Chemosphere* 262 (2021) 128376, <https://doi.org/10.1016/j.chemosphere.2020.128376>.
- [52] S.S. Oncel, A. Kose, D.Ş. Oncel, Carbon sequestration in microalgae photobioreactors building integrated, in: *Start-Up Creat*, Elsevier, 2020, pp. 161–200, <https://doi.org/10.1016/b978-0-12-819946-6.00008-4>.
- [53] M. Kerner, Optimization of sound insulation of flat panel photobioreactors for bioenergy façades, *Archit. Struct. Constr.* (2023), <https://doi.org/10.1007/s44150-023-00085-w>.
- [54] N. Boloria, Y. Thakkar, Integrating algae building technology in the built environment: a cost and benefit perspective, *Front. Archit. Res.* 9 (2020) 370–384, <https://doi.org/10.1016/j.foar.2019.12.004>.
- [55] J. Pruvost, F. Le Borgne, A. Artu, J.F. Cornet, J. Legrand, Industrial photobioreactors and scale-up concepts, *Adv. Chem. Eng.* 48 (2016) 257–310, <https://doi.org/10.1016/bs.ache.2015.11.002>.
- [56] M. Raeesossadi, N.R. Moheimani, D. Parlevliet, Luminescent solar concentrator panels for increasing the efficiency of mass microalgal production, *Renew. Sustain. Energy Rev.* 101 (2019) 47–59, <https://doi.org/10.1016/j.rser.2018.10.029>.
- [57] A. Mazzelli, A. Cicci, F. Di Caprio, P. Altimari, L. Toro, G. Iaquaniello, F. Pagnanelli, Multivariate modeling for microalgae growth in outdoor photobioreactors, *Algal Res.* 45 (2020) 101663, <https://doi.org/10.1016/j.algal.2019.101663>.
- [58] M.A. Borowitzka, Limits to growth, in: Y.-S.W.F.Y. Tam (Ed.), *Wastewater Treat. With Algae*. Biotechnol. Intell. Unit, Springer, Berlin, Heidelberg, 1998, pp. 203–226, [https://doi.org/10.1007/978-3-662-10863-5\\_12](https://doi.org/10.1007/978-3-662-10863-5_12).
- [59] M. Kerner, T. Gebken, I. Sundarrao, S. Hindersin, D. Sauss, Development of a control system to cover the demand for heat in a building with algae production in a bioenergy façade, *Energy Build.* 184 (2019) 65–71, <https://doi.org/10.1016/j.enbuild.2018.11.030>.
- [60] S. Wilkinson, P. Stoller, P. Ralph, B. Hamdorf, L.N. Catana, G.S. Kuzava, Exploring the feasibility of algae building technology in NSW, *Procedia Eng.* 180 (2017) 1121–1130, <https://doi.org/10.1016/j.proeng.2017.04.272>.
- [61] E. Negev, A. Yezioro, M. Polikovsky, A. Kribus, J. Cory, L. Shashua-Bar, A. Golberg, Algae Window for reducing energy consumption of building structures in the Mediterranean city of Tel-Aviv, Israel, *Energy Build.* 204 (2019) 109460, <https://doi.org/10.1016/j.enbuild.2019.109460>.
- [62] M. Talei, M. Mahdavejad, R. Azari, A. Prieto, H. Sangin, Multi-objective optimization of building-integrated microalgae photobioreactors for energy and daylighting performance, *J. Build. Eng.* 42 (2021) 102832, <https://doi.org/10.1016/j.jobe.2021.102832>.
- [63] M. Talei, M. Mahdavejad, R. Azari, H.M. Haghghi, A. Atashdast, Thermal and energy performance of a user-responsive microalgae bioreactive façade for climate adaptability, *Sustain. Energy Technol. Assessments* 52 (2022) 101894, <https://doi.org/10.1016/j.seta.2021.101894>.
- [64] V.R.M. Lo Verso, M.H.S. Javadi, S.L. Pagliolico, C. Carbonaro, G. Sassi, Photobioreactors as a dynamic shading system conceived for an outdoor workspace of the state library of queensland in brisbane: study of daylighting performances, *J. Daylighting.* 6 (2019) 148–168, <https://doi.org/10.15627/jd.2019.14>.
- [65] M. Talei, M. Mahdavejad, Probable cause of damage to the panel of microalgae bioreactor building façade: hypothetical evaluation, *Eng. Fail. Anal.* 101 (2019) 9–21, <https://doi.org/10.1016/j.engfailanal.2019.02.060>.
- [66] C.F. Reinhart, O. Walkenhorst, Validation of dynamic RADIANCE-based daylight simulations for a test office with external blinds, *Energy Build.* 33 (2001) 683–697, [https://doi.org/10.1016/S0378-7788\(01\)00058-5](https://doi.org/10.1016/S0378-7788(01)00058-5).
- [67] C. Reinhart, B. Pierre-Felix, Experimental validation of autodesk® 3ds max® design 2009 and daysim 3.0, *LEUKOS - J. Illum. Eng. Soc. North Am.* 6 (2009) 7–35, <https://doi.org/10.1582/LEUKOS.2009.06.01001>.
- [68] M.J. Witte, R.H. Henninger, J. Glazer Gard Analytics, D.B. Crawley, Testing and validation of a new building energy simulation program, *Seventh Int. IBPSA Conf.* (2001) 353–360, <https://simulationresearch.lbl.gov/dirpubs/rio4.pdf>.
- [69] R. Henninger, Experience testing energyplus with the IEA HVAC BESTest e100-e200 series, *Proc. 8th Int. IBPSA Conf.* (2003) 467–474, [http://simulationresearch.lbl.gov/dirpubs/BS03/bs03\\_04.pdf](http://simulationresearch.lbl.gov/dirpubs/BS03/bs03_04.pdf).
- [70] X. Zhou, R. Liu, S. Tian, X. Shen, X. Yang, J. An, D. Yan, A review of validation methods for building energy modeling programs, *Build. Simulat.* 16 (2023) 2027–2047, <https://doi.org/10.1007/s12273-023-1050-0>.
- [71] A. Zhang, Y. Li, Thermal conductivity of Aluminum alloys—a review, *Materials* 16 (2023), <https://doi.org/10.3390/ma16082972>.
- [72] L. Bellia, F. De Falco, F. Minichiello, Effects of solar shading devices on energy requirements of standalone office buildings for Italian climates, *Appl. Therm. Eng.* 54 (2013) 190–201, <https://doi.org/10.1016/j.applthermaleng.2013.01.039>.
- [73] Y. Fang, S. Cho, Design optimization of building geometry and fenestration for daylighting and energy performance, *Sol. Energy* 191 (2019) 7–18, <https://doi.org/10.1016/j.solener.2019.08.039>.
- [74] Y. Geng, B. Lin, Y. Zhu, Comparative study on indoor environmental quality of green office buildings with different levels of energy use intensity, *Build. Environ.* 168 (2020) 106482, <https://doi.org/10.1016/j.buildenv.2019.106482>.
- [75] P. Shen, Z. Wang, How neighborhood form in fl uences building energy use in winter design condition : case study of Chicago using CFD coupled simulation, *J. Clean. Prod.* 261 (2020) 121094, <https://doi.org/10.1016/j.jclepro.2020.121094>.
- [76] A. Nabil, J. Mardaljevic, Useful daylight illuminance: a new paradigm for assessing daylight in buildings, *Light. Res. Technol.* 37 (2005) 41–59, <https://doi.org/10.1191/1365782805li128oa>.
- [77] A. Tabadkani, A. Roetzal, X. Li, Daylight in Buildings and Visual Comfort Evaluation : the Advantages and Limitations, vol. 8, 2021, pp. 181–203, <https://doi.org/10.15627/jd.2021.16>.
- [78] E. Brembilla, J. Mardaljevic, Climate-Based Daylight Modelling for compliance verification: benchmarking multiple state-of-the-art methods, *Build. Environ.* 158 (2019) 151–164, <https://doi.org/10.1016/j.buildenv.2019.04.051>.
- [79] M.E. Emeter, Typical environmental challenges, *Numer. Methods Environ. Data Anal.* (2022) 41–51, <https://doi.org/10.1016/b978-0-12-818971-9.00004-1>.
- [80] ANSI/ASHRAE Standard 55, *Thermal Environmental Conditions for Human Occupancy*, 2013.
- [81] ISO 7730-2005 Ergonomics of the Thermal Environment-Analytical Determination and Interpretation of Thermal Comfort Using Calculation of the PMV and PPD Indices and Local Thermal Comfort Criteria, 2005.
- [82] T. Cheung, S. Schiavon, T. Parkinson, P. Li, G. Brager, Analysis of the accuracy on PMV – PPD model using the ASHRAE global thermal comfort database II, *Build. Environ.* 153 (2019) 205–217, <https://doi.org/10.1016/j.buildenv.2019.01.055>.
- [83] ASHRAE Standard, 55-201 7-Thermal Environmental Conditions for Human Occupancy, 55–201 7, ANSI/ASHRAE Stand, 2017.
- [84] R. Wang, S. Lu, W. Feng, Impact of adjustment strategies on building design process in different climates oriented by multiple performance, *Appl. Energy* 266 (2020) 114822, <https://doi.org/10.1016/j.apenergy.2020.114822>.

- [85] C. Sun, Q. Liu, Y. Han, Many-objective optimization design of a public building for energy, daylighting and cost performance improvement, *Appl. Sci.* 10 (2020), <https://doi.org/10.3390/app10072435>.
- [86] F. Yang, D. Bouchlaghem, Genetic algorithm-based multiobjective optimization for building design, *Architect. Eng. Des. Manag.* 6 (2010) 68–82, <https://doi.org/10.3763/aedm.2008.0077>.
- [87] N. Gunantara, A review of multi-objective optimization: methods and its applications, *Cogent Eng.* 5 (2018) 1–16, <https://doi.org/10.1080/23311916.2018.1502242>.
- [88] N. Gunantara, G. Hendranto, Multi-Objective cross-Layer optimization for selection of cooperative path Pairs in multihop wireless Ad hoc networks, *J. Commun. Softw. Syst.* 9 (2013) 170–177.
- [89] X.-S. Yang, Multi-objective optimization, in: *Nature-Inspired Optim. Algorithms*, Elsevier, 2014, pp. 197–211, <https://doi.org/10.1016/B978-0-12-416743-8.00014-2>.
- [90] N. Brown, J. Ochsendorf, C. Mueller, J. de Oliveira, Early-stage integration of architectural and structural performance in a parametric multi-objective design tool, *Struct. Archit. - Proc. 3rd Int. Conf. Struct. Archit. ICSA 2016* (2016) 1103–1111, <https://doi.org/10.1201/b20891-152>.
- [91] E. Zitzler, M. Laumanns, L. Thiele, SPEA2: improving the Strength pareto evolutionary algorithm, *Evol. Methods Des. Optim. Control with Appl. to Ind. Probl.* (2001) 95–100.
- [92] J. Bader, E. Zitzler, HypE: an algorithm for fast hypervolume-based many-objective optimization, *Evol. Comput.* 19 (2011) 45–76.
- [93] Y. Cao, B.J. Smucker, T.J. Robinson, On using the hypervolume indicator to compare Pareto fronts: applications to multi-criteria optimal experimental design, *J. Stat. Plann. Inference* 160 (2015) 60–74, <https://doi.org/10.1016/j.jspi.2014.12.004>.
- [94] M.C. Toklu, The Technique for Order of Preference by Similarity to Ideal Solution Method in Fuzzy Environment, Springer International Publishing, 2020, <https://doi.org/10.4018/978-1-7998-2216-5.ch007>.
- [95] C.-L. Hwang, K. Yoon, *Multiple Attribute Decision Making*, Springer Berlin, Heidelberg, 1981, <https://doi.org/10.1007/978-3-642-48318-9>.
- [96] J.J. Thakkar, Linear programming techniques for multidimensional analysis of preference (LINMAP), in: *Stud. Syst. Decis. Control*, Springer Science and Business Media Deutschland GmbH, 2021, pp. 199–218, [https://doi.org/10.1007/978-981-33-4745-8\\_12/COVER](https://doi.org/10.1007/978-981-33-4745-8_12/COVER).
- [97] N.H. Son, T.T. Hieu, N.M. Thang, H.N. Tan, N.T. Can, P.T. Thao, N.C. Bao, Choosing the best machine tool in mechanical manufacturing, *EUREKA, Phys. Eng.* 2023 (2023) 97–109, <https://doi.org/10.21303/2461-4262.2023.002771>.
- [98] B. Uzun, A. Almasri, D. Uzun Ozsahin, Preference ranking organization method for enrichment evaluation (promethee), in: D. Uzun Ozsahin, H. Gökçekuş, B. Uzun, J. LaMoreaux (Eds.), *Appl. Multi-Criteria Decis. Anal. Environ. Civ. Eng.*, Springer, Cham, 2021, pp. 37–41, [https://doi.org/10.1007/978-3-030-64765-0\\_6](https://doi.org/10.1007/978-3-030-64765-0_6).
- [99] M. Sharafi, T.Y. Elmekawy, Multi-objective optimal design of hybrid renewable energy systems using PSO-simulation based approach, *Renew. Energy* 68 (2014) 67–79, <https://doi.org/10.1016/j.renene.2014.01.011>.
- [100] T. Niknam, M. Bornapour, A. Gheisari, Combined heat, power and hydrogen production optimal planning of fuel cell power plants in distribution networks, *Energy Convers. Manag.* 66 (2013) 11–25, <https://doi.org/10.1016/J.ENCONMAN.2012.08.016>.
- [101] Z. Wang, G.P. Rangaiah, Application and analysis of methods for selecting an optimal solution from the Pareto-Optimal Front obtained by multiobjective optimization, *Ind. Eng. Chem. Res.* 56 (2017) 560–574, <https://doi.org/10.1021/acs.iecr.6b03453>.
- [102] N. Delgarm, B. Sajadi, S. Delgarm, Multi-objective optimization of building energy performance and indoor thermal comfort: a new method using artificial bee colony (ABC), *Energy Build.* 131 (2016) 42–53, <https://doi.org/10.1016/j.enbuild.2016.09.003>.
- [103] G.R. Jahanshaloo, F.H. Lotfi, M. Izadikhah, An algorithmic method to extend TOPSIS for decision-making problems with interval data, *Appl. Math. Comput.* 175 (2006) 1375–1384, <https://doi.org/10.1016/j.amc.2005.08.048>.
- [104] R.A. Krohling, V.C. Campanharo, Fuzzy TOPSIS for group decision making: a case study for accidents with oil spill in the sea, *Expert Syst. Appl.* 38 (2011) 4190–4197, <https://doi.org/10.1016/j.eswa.2010.09.081>.
- [105] S.S. Oncel, A. Kose, D.Ş. Oncel, Façade integrated photobioreactors for building energy efficiency, in: F. Pacheco-Torgal, E. Rasmussen, C.-G. Granqvist, V. Ivanov, A. Kaklauskas, S. Makonin (Eds.), *Start-Up Creat. Smart Eco-Efficient Built Environ*, Woodhead Publishing, 2016, pp. 237–299, <https://doi.org/10.1016/B978-0-08-100546-0.00011-X>.
- [106] J. Wurm, Photobioreactors on façades for energy generation *Alternative technologies in the building envelope*, *Int. Rosenheim Wind. Facadefacade Conf. 2013* (2013) 83–87.
- [107] N.C. Brown, V. Jusiega, C.T. Mueller, Implementing data-driven parametric building design with a flexible toolbox, *Autom. Construct.* 118 (2020) 103252, <https://doi.org/10.1016/j.autcon.2020.103252>.
- [108] Z. Pang, Z. O'Neill, Y. Li, F. Niu, The role of sensitivity analysis in the building performance analysis: a critical review, *Energy Build.* 209 (2020) 109659, <https://doi.org/10.1016/j.enbuild.2019.109659>.
- [109] B. Iooss, P. Lemaître, A review on global sensitivity analysis methods, *Oper. Res. Comput. Sci. Interfaces Ser.* 59 (2015) 101–122, <https://doi.org/10.1007/978-1-4899-7547-8>.
- [110] T. Wei, A review of sensitivity analysis methods in building energy analysis, *Renew. Sustain. Energy Rev.* 20 (2013) 411–419, <https://doi.org/10.1016/j.rser.2012.12.014>.
- [111] P. Hoseinzadeh, M. Khalaji, S. Heidari, M. Khalatbari, R. Saidur, K. Haghighat, H. Sangin, Energy performance of building integrated photovoltaic high-rise building : case study , Tehran , Iran, *Energy Build.* 235 (2021) 110707, <https://doi.org/10.1016/j.enbuild.2020.110707>.
- [112] M.T. Aguilar-Carrasco, F. Díaz-Borrego, I. Acosta, M.Á. Campano, S. Domínguez-Amarillo, Validation of lighting parametric workflow tools of Ladybug and Solemma using CIE test cases, *J. Build. Eng.* 64 (2023), <https://doi.org/10.1016/j.jobbe.2022.105608>.
- [113] F. Kharvari, An empirical validation of daylighting tools: assessing radiance parameters and simulation settings in Ladybug and Honeybee against field measurements, *Sol. Energy* 207 (2020) 1021–1036, <https://doi.org/10.1016/j.solener.2020.07.054>.
- [114] F. Kharvari, A field-validated multi-objective optimization of the shape and size of windows based on daylighting metrics in hot-summer mediterranean and dry summer continental climates, *J. Daylighting.* 7 (2020) 222–237, <https://doi.org/10.15627/jd.2020.19>.
- [115] E.S. Lee, D. Geisler-Moroder, G. Ward, Modeling the direct sun component in buildings using matrix algebraic approaches: methods and validation, *Sol. Energy* 160 (2018) 380–395, <https://doi.org/10.1016/j.solener.2017.12.029>.
- [116] M. Tavakolan, F. Mostafazadeh, S. Jalilzadeh Eirdmoussa, A. Safari, K. Mirzaei, A parallel computing simulation-based multi-objective optimization framework for economic analysis of building energy retrofit: a case study in Iran, *J. Build. Eng.* 45 (2022) 103485, <https://doi.org/10.1016/j.jobbe.2021.103485>.

## Nomenclature

- A<sup>+</sup>: Positive ideal solutions  
 A: Negative ideal solutions  
 ABBS: Algae-based bioshading systems  
 ANN: Artificial neural network  
 ASE: Annual Sunlight Exposure  
 ATC: Adaptive thermal comfort  
 Aw: Tropical savanna  
 B: Best  
 BPS: Building Performance Simulation  
 BSh: Hot semi-arid  
 BSK: Cold semi-arid  
 BWh: Hot desert climate

*Cfa*: Humid subtropical  
*Csa*: Hot-summer Mediterranean  
*CTR*: Annual thermal comfort ratio  
*DA*: Daylight Autonomy  
*Dfb*: Humid continental  
*DGP*: Daylight Glare Probability  
*E<sub>Daylight</sub>*: Daylight  
*EU<sub>i</sub>*: Energy demand  
*EUI*: Energy Usage Intensity  
*EUI<sub>Cooling</sub>*: Cooling EUI  
*EUI<sub>Equipment</sub>*: Equipment EUI  
*EUI<sub>Heating</sub>*: Heating EUI  
*EUI<sub>Lighting</sub>*: Lighting EUI  
*f(x)*: Objective function  
*FESD*: Fixed exterior shading device  
*FUCA*: Faire un choix adequat  
*HypE*: Hypervolume Estimation Algorithm  
*IOT*: Indoor operative temperature  
*J*: Set of maximization objective  
*J'*: Set of minimization objective  
*LINMAP*: Linear programming technique for multidimensional analysis of preference  
*MLR*: Multiple linear regression  
*MOO*: Multi-objective optimization  
*MOGA*: Multi-objective genetic algorithm  
*MOPSO*: Multi-objective particle swarm optimization  
*MW*: Microalgae window  
*n*: Number of objective functions  
*N<sub>e</sub>*: Annual equipment hours  
*N<sub>c</sub>*: Annual cooling hours  
*N<sub>h</sub>*: Annual heating hours  
*N<sub>l</sub>*: Annual lighting hours  
*NSGA-II*: Non-dominated sorting genetic algorithm II  
*OAT*: Outdoor air temperature  
*OF*: Overhang with fin  
*PROMETHEE II*: Preference ranking organization method for enrichment of evaluations II  
*PCM*: Phase Changing Material  
*PBR*: Photobioreactor  
*PBRF*: Photobioreactor Facades  
*POF*: Pareto optimal front  
*PT*: Proportion of thermal comfort duration  
*PMV*: Predicted mean vote  
*PPD*: Percentage of people dissatisfied  
*q*: Total hour  
*r*: Reference point  
*SA*: Side angle  
*S<sub>i+</sub>*: Euclidean distance from positive ideal solutions  
*S<sub>i-</sub>*: Euclidean distance from negative ideal solutions  
*SDA*: Spatial daylight autonomy  
*sDG*: Spatial Disturbing Glare  
*sDVA*: Spatial daylight vote autonomy  
*sGA*: Spatial glare autonomy  
*SHGC*: Solar heat gain coefficient  
*SPEA-II*: Strength Pareto Evolutionary Algorithm  
*SRC*: Standardized Regression Coefficients  
*SRC<sub>j</sub><sup>2</sup>*: Share of variance  
*T*: Indoor operative temperature (IOT)  
*T<sub>co</sub>*: Indoor comfort temperature  
*t<sub>i</sub>*: Time fraction  
*T<sub>Lo</sub>*: Lower air temperature  
*T<sub>ref</sub>*: Mean outdoor air temperature  
*T<sub>Up</sub>*: Upper air temperature  
*TA*: Top angle  
*TCP*: Thermal Comfort Percentage  
*TES*: Annual total power consumption  
*TEUI*: Thermal energy use intensity  
*TOPSIS*: Technique for Order of Preference by Similarity to Ideal Solution  
*U*: Feasible set  
*UDI*: Useful Daylight Illuminance  
*UDI<sub>overlit</sub>*: Upper thresholds  
*UDI<sub>underlit</sub>*: Lower threshold  
*UDI<sub>useful</sub>*: Acceptable range  
*USRC*: Unstandardized Regression Coefficient  
*v*: Criterion vector  
*v<sub>ij</sub>*: Weighted normalized value  
*VT*: Visible light transmittance  
*w*: Weighting coefficient  
*w<sub>j</sub>*: Weight of the *i*th attribute/criterion  
*w<sub>fj</sub>*: Weighting factor  
*WWR*: Window-to-wall ratio  
*x*: MOO solutions

$X_j$ : Variable

$Y$ : Output

$\beta_j$ : Linear regression coefficient

$\lambda$ : Lebesgue measure